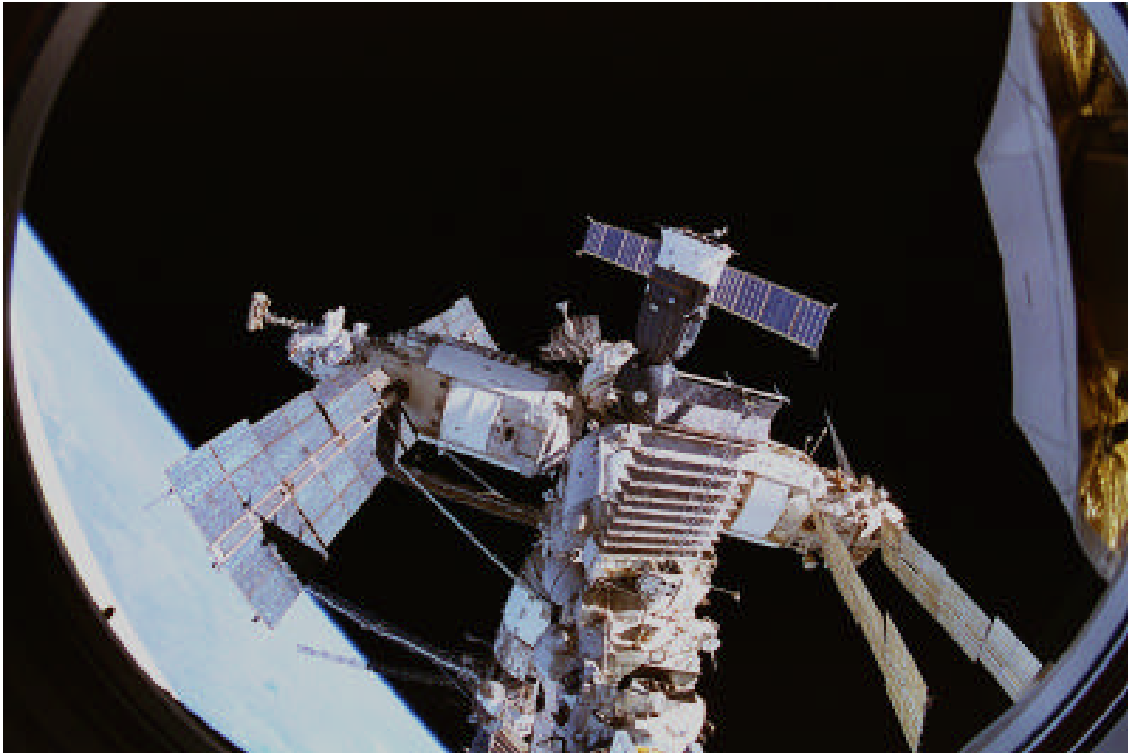


Mir Photo/TV Survey (DTO-1118): STS-84 Mission Report



Prepared by:
**Image Science and Analysis Group
Earth Science Branch
Earth Science and Solar System Exploration Division**

September 1997

ACKNOWLEDGMENTS

This document was prepared by Image Science & Analysis Group (IS&AG) personnel in the Earth Science Branch, Earth Science and Solar System Exploration Division. Mike Gaunce/NASA/JSC, Robert Scharf/LMES, Teresa Morris/LMES, Vince Elliott/LMES, Kevin Crosby/LMES and Jim Dragg/LMES have all made contributions to the preparation and analysis that have gone into this report. Kurt Bush/SP/LMES provided invaluable assistance in generating CAD images used in the resolution of camera field-of-view issues and crew training documents during the months leading up to STS-84. Pete Counihan/MS2/RSO and Dominic Ngan/Rockwell-Downey provided much of the information on the Mir Station configuration changes. Thomas Kerslake/LeRC provided information on the size and structure of Mir solar cells. Eric Christiansen/NASA/JSC provided descriptive information on the form and structure of the micrometeoroid and orbital debris strikes. Thanks are given to the film and video personnel in the Imagery & Publications Office/BT4 without whose help many extra hours of sorting through data would have been required. Special thanks to Judy Alexander/DF43/RSO and Don Carico/DF43/RSO for helping integrate DTO-1118 requirements into the crew training documentation. We would like to acknowledge the STS-84 crew for gathering the photographic and video data and the Instrumentation and Communications Officers (INCO) in Mission Control for their support in obtaining ground-controlled video. Finally, the support of the ISS Phase 1 Program is gratefully acknowledged. Many other individuals (too numerous to name) from various science, engineering, and operations groups have made contributions to the knowledge gathered and presented in this final report.

Questions about the contents of this document should be addressed to Mike Gaunce, JSC Code SN5, at 281-483-5153 or Robert Scharf, Lockheed Martin Code C23, at 281-483-2756.

EXECUTIVE SUMMARY

NASA and the Russian Space Agency are involved in a cooperative venture in which the Shuttle will rendezvous and dock with the Mir Space Station during several missions from 1995 to 1998. This sequence of nine missions will serve as a precursor to the two nations' involvement in the International Space Station. These joint missions provide NASA scientists and engineers an opportunity to study the orbital, dynamic, and environmental conditions of long-duration spacecraft, as well as develop evaluation and risk mitigation techniques which have direct application to the International Space Station.

STS-84 was the Shuttle's seventh rendezvous with, and sixth docking to, Mir. It was launched on May 15, 1997 and was docked to Mir from May 17 to May 22, 1997. STS-84 was the first Mir flight which did not have a fly-around and imagery survey of the Mir.

Detailed Test Objective 1118 (DTO-1118) integrates the requirements for photographic and video imagery of Mir generated by the engineering, operations, and science communities within NASA. Although mission requirements vary, the principal objectives of the DTO-1118 Mir Photo/TV Surveys are as follows:

- Study the effects of the space environment on a long-duration orbiting platform.
- Assess the overall condition of the Mir.
- Provide assurance of crew and Shuttle safety while in the proximity of the Mir Space Station.
- Analyze the dynamic effects of structures and appendages (e.g., solar array motion).
- Understand the impact of plume impingement during proximity operations.
- Evaluate the equipment and procedures used to gather survey data.

This report documents the results from STS-84 survey-related imagery analysis tasks. Reports of previous Mir surveys are listed in Section 11, References.

Summary of Findings

Approximately 1000 photographs and 13 hours of video of the Mir Space Station were acquired during the STS-84 mission. The significant findings from the analyses of still photography and video from this mission are as follows:

- No new damage was identified on Mir surfaces that had not been observed on previous Shuttle flights. However, additional details were observed of micrometeoroid/orbital debris damage and discolorations/depositions of Mir surfaces.
- The configuration of the Mir Space Station for STS-84 was essentially the same as it was for STS-81. The new addition to Mir was the Optical Properties Monitor attached to the Docking Module. Section 2 identifies the Mir modules photographed during STS-84.

-
- Micrometeoroid and Orbital Debris (MMOD) strikes were described, measured, and counted from the STS-84 high resolution photography. Analysis of MMOD strikes were performed for portions of the Docking Module, Kvant-2 radiator, and the Kristall SP#2, Base Block SP#2, and Kvant-2 SP#2 solar arrays. Strikes as small as 0.6 mm and damage areas as large as 8 cm x 10 cm have been shown. Results and images are provided in Section 3.
 - Deposition/discoloration in the form of a “wake” or “shadowing” effect was detected on the thermal blanket on the end of the newly-deployed Optical Properties Monitor which had been installed on the Docking Module less than one month prior to the mission. Section 3 contains the images and analysis results.
 - A possible leak on the Spektr radiator, discovered during STS-81, was photographed on STS-84. The stain from the leak showed only a small increase in size between STS-81 and STS-84. The stain is shown in Section 3, Figure 3.14.
 - The capture and structural latches of the Mir Docking Module docking mechanism were shown to be in proper position before docking and after separation. The laser retroreflectors and electrical connectors appeared to be in good physical condition, however the imagery was not of sufficient resolution to detect any discoloration which might exist. See Section 4.
 - Video imagery was obtained of the Base Block SP#2 array in response to four sequences of Shuttle thruster firings. Motion of the array was detectable in the video of only one of the thruster firing sequences. Video of this motion was used to measure peak-to-peak deflections and dominant frequencies. The peak-to-peak deflections were 0.14 ± 0.10 inches for out-of-plane motion and 0.27 ± 0.07 inches for in-plane motion. The dominant frequency for in-plane motion was approximately 0.24 Hz, and approximately 0.27 Hz for out-of-plane motion. Results were provided to the MiSDE principal investigator for modal analysis in support to ISS Photovoltaic Array Analysis. A description of the issues, analyses, and results are provided in Section 5.
 - Two pieces of debris were observed after the Shuttle made docking contact with Mir. One piece of debris, approximately 4.3 cm in size, made contact with the Reusable Solar Array carrier thermal blanket, which deflected the path and reduced the velocity of the debris. High-resolution film imagery, taken later during the mission, did not show any damage from the debris contact. See Section 6.
 - No damage or discoloration was observed on the Mir Environmental Effects Payload (MEEP) experiment panels. Images of the panels are shown in Section 7.
 - The position of the Kurs antenna attached to the Mir Docking Module was determined in Shuttle coordinates. This analysis was performed in support of projected clearance calculations between the antenna and the Shuttle forward bulkhead for the planned STS-91 mission to be launched in May 1998. The results did not significantly change from the measurements made from STS-81 imagery. See Section 8.
 - The overall quality of the imagery from STS-84 was excellent. The crew acquired detailed imagery using the 35 mm camera with 400 mm lens and 2X

extender lens while docked. The increased scale provided by the 2X lens supported detailed analyses. Payload Bay Camera C developed a smudge (possibly due to condensation) in the center of the lens during the mission. The smudge affected the quality of the survey imagery from that camera. See Section 9.

Additional conclusions and recommendations are included in Section 10 of this mission report.

Table of Contents

1. INTRODUCTION.....	1
2. MIR CONFIGURATION	2
3. MIR SURFACE ASSESSMENT.....	4
3.1 Micrometeoroid and Orbital Debris Damage Assessment.....	4
3.2 Surface Deposition and Discoloration.....	16
4. DOCKING MECHANISM ASSESSMENT	22
5. MIR STRUCTURAL DYNAMICS EXPERIMENT SOLAR ARRAY MOTION. 24	
5.1 Solar Array Video Data Acquisition.....	24
5.2 Data Analysis Approach.....	27
5.3 Results	27
6. DEBRIS DURING DOCKING OPERATIONS.....	32
7. MIR ENVIRONMENTAL EFFECTS PAYLOAD ASSESSMENT.....	35
8. POSITION OF THE KURS ANTENNA ATTACHED TO THE DOCKING MODULE.....	38
9. IMAGERY EVALUATION	41
9.1 Still Photography Review.....	41
9.2 Video Review.....	42
9.3 Crew Assessments.....	43
10. CONCLUSIONS AND RECOMMENDATIONS.....	45
10.1 Conclusions.....	45
10.2 Recommendations	45
11. REFERENCES	47
12. ACRONYMS & ABBREVIATIONS	48

APPENDICES

Appendix A:	STS-84 Film Scenelist
Appendix B:	STS-84 Video Scenelist
Appendix C:	Sources for Report Imagery
Appendix D:	STS-84 Camera Layout

List of Figures

Figure 2.1	Mir Space Station.....	2
Figure 2.2	Docking Module	3
Figure 3.1	Typical View and Cross Section of MMOD Strike.....	5
Figure 3.2	Kristall SP#2 MMOD Strikes.....	7
Figure 3.3	Base Block SP#2 MMOD Strikes.....	8
Figure 3.4	Circular MMOD Strike Pattern on Base Block SP#2.....	9
Figure 3.5	MMOD Strikes on Kvant-2 SP#2.....	10
Figure 3.6	A View of the Back Side of Kvant-2 SP#2 MMOD Strike.....	11
Figure 3.7	Possible MMOD Strikes on a Portion of Kvant-2 Radiator.....	12
Figure 3.8	Possible MMOD strikes on Docking Module Thermal Blanket	13
Figure 3.9	Deposition on Base of RSA Carrier.....	17
Figure 3.10	Irregularity on Surface of an RSA Carrier Hinge.....	17
Figure 3.11	Discoloration and Possible Stain on Docking Module Thermal Blanket .	18
Figure 3.12	Docking Module - ROEU-PDA.....	19
Figure 3.13	Docking Module - OPM.....	20
Figure 3.14	Progress of Possible Leak on Spektr Radiator	21
Figure 4.1	Photo of Docking Mechanism during Approach.....	22
Figure 4.2	Video of Docking Mechanism during Backaway.....	23
Figure 5.1	A Multiplexed Video Frame Used in the Motion Analysis of Base Block SP#2	26
Figure 5.2	Out-of-Plane Deflection of Base Block SP#2	29
Figure 5.3	In-Plane Deflection of Base Block SP#2	29
Figure 5.4	Out-of-Plane Frequency of Base Block SP#2	30
Figure 5.5	In-Plane Frequency of Base Block SP#2	30
Figure 6.1	Debris Observed Making Contact with RSA Carrier at GMT 137d:02h:36m:28s.....	33
Figure 6.2	Spherical Debris Observed between PLB Camera C and Mir Docking Module at GMT 137d:02h:39m:54s	34
Figure 7.1.	STS-84 Image of Mir with MEEP Experiments.....	35
Figure 7.2	Image of POSA Acquired from Aft Flight Deck Window.....	36
Figure 7.3	Images of Panels on Both Sides of POSA II.....	36
Figure 7.4	Images of ODC and PPMD	37
Figure 8.1	Kurs Antenna as seen from the Shuttle Flight Deck on STS-84	38
Figure 8.2	Kurs Antenna as seen from Payload Bay Camera A	39

List of Figures

Figure 8.3 Kurs Antenna as seen from Payload Bay Camera D 39

List of Tables

Table 3-1	Size Distribution of MMOD Strikes from STS-84 Images.....	15
Table 5-1	Shuttle Thruster Firing Sequences for MiSDE.....	26
Table 8-1	Coordinates of Kurs Antenna Tip.....	40

1. INTRODUCTION

As part of DTO-1118, approximately 1000 photographs and 13 hours of video of the Mir Space Station were acquired during the STS-84 mission.

The Image Science & Analysis Group (IS&AG) conducted several analysis tasks (based on user requirements) using the imagery data from STS-84. The purpose of the analysis tasks were to:

- Verify the configuration of the Mir complex.
- Assess the effect of micrometeoroid impacts and other visible damage on Mir surfaces.
- Compare the condition of Mir external surfaces to that seen on previous missions.
- Measure the motion of the Mir Base Block SP#2 in response to prescribed firings of Shuttle thrusters while the Shuttle was docked to Mir.
- Document the condition of the docking mechanism.
- Characterize debris seen during and after docking operations.
- Determine the position of the Kurs antenna attached to the Mir Docking Module (DM) in relation to the Shuttle for potential clearance issues on the subsequent STS-91 docking mission.
- Assess the quality of video and photographic data.

The following sections of this mission report describe the analyses, results, conclusions and recommendations from STS-84.

2. MIR CONFIGURATION

The configuration of the Mir Space Station for STS-84 was essentially the same as it was for STS-81. The new addition to Mir was the Optical Properties Monitor (OPM) attached to the Docking Module.

Information on the Mir configuration is important for proximity operations requiring visual navigation and for conducting simulations of structural loads on docked configurations. Available drawings of the Mir Space Station were compared to photography acquired during the rendezvous. The Shuttle approach view in Figure 2.1 identifies different Mir modules photographed during STS-84. The approach view in Figure 2.2 identifies the location of OPM, the only new feature added to the Mir Station.

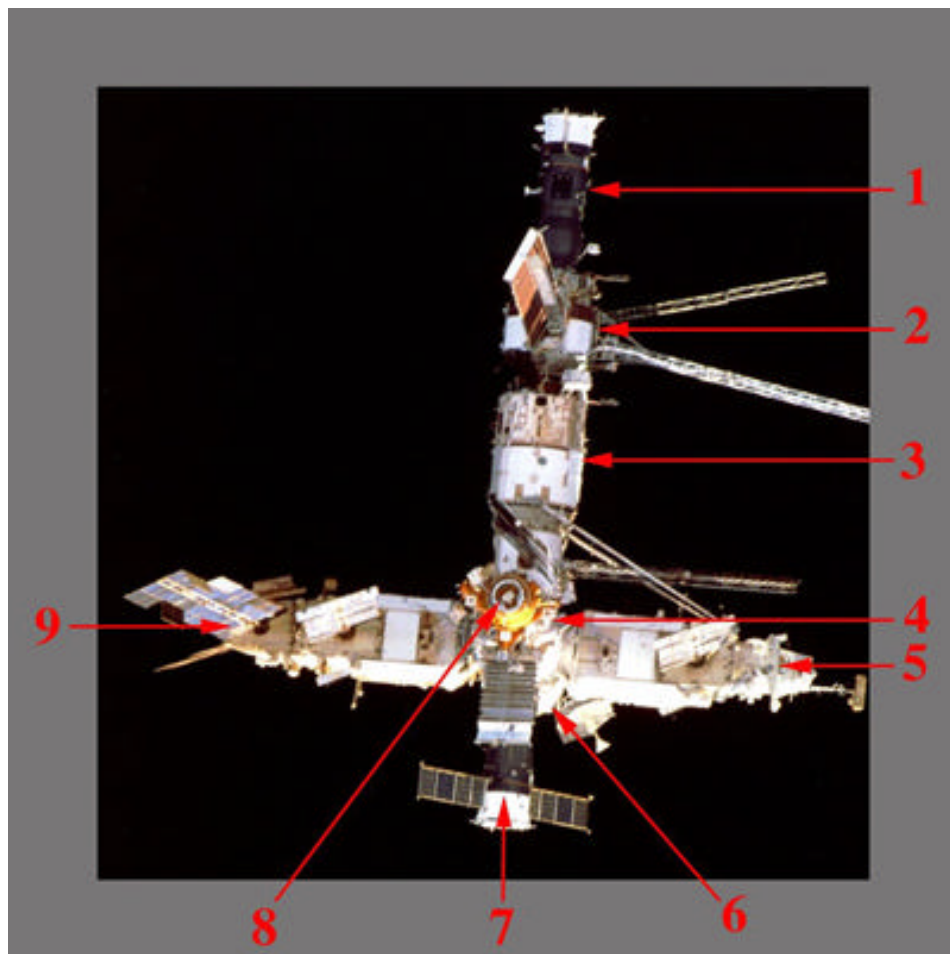


Figure 2.1 Mir Space Station

- | | |
|---------------|-------------------------|
| 1. Progress | 6. Priroda (obstructed) |
| 2. Kvant | 7. Soyuz |
| 3. Base Block | 8. Docking Module |
| 4. Kristall | 9. Spektr |
| 5. Kvant-2 | |

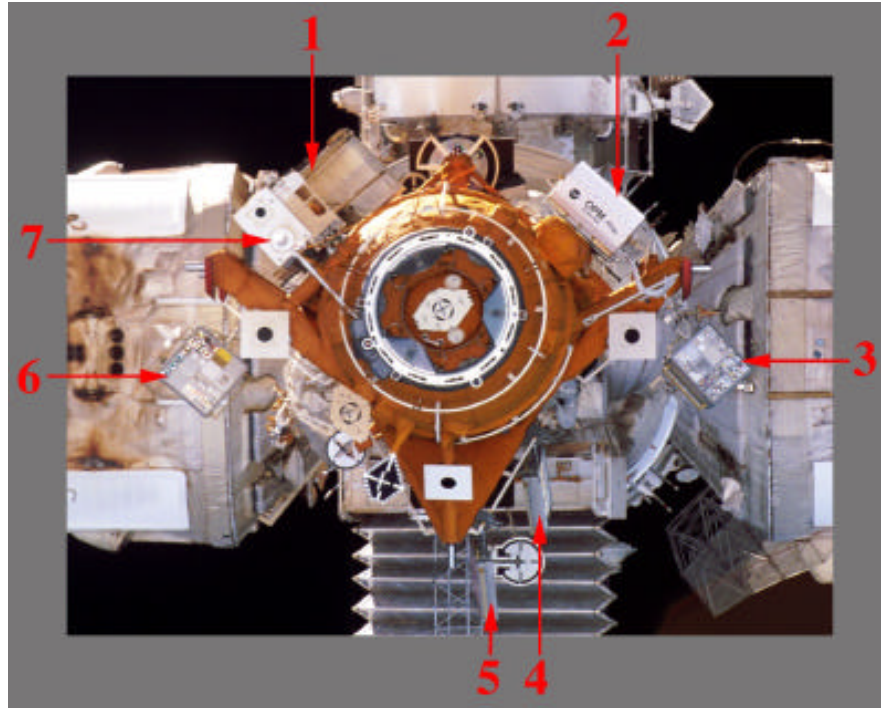


Figure 2.2 Docking Module

- 1. Reusable Solar Array (RSA)**
- 2. Optical Properties Monitor (OPM)**
- 3. Passive Optical Sample Assembly II (POSA II)**
- 4. Polished Plate Micrometeoroid & Debris (PPMD) Experiment**
- 5. Orbital Debris Collector (ODC) Experiment**
- 6. Passive Optical Sample Assembly (POSA)**
- 7. Kurs Antenna**

3. MIR SURFACE ASSESSMENT

An assessment was performed of the DTO-1118 survey imagery of visible Mir Station components taken during STS-84. As on other Mir missions, chipped and peeling paint was noted on Spektr radiator and RSA (Reusable Solar Array) surfaces. Detailed video coverage of the RSA carrier on the Docking Module shows peeling paint on different areas of the supporting truss structure of the RSA.

The pattern of discoloration has not significantly changed. Surface discoloration was observed around all of the visible module mooring and stabilization engines. Discoloration was noted near the docking node of the Base Block. Also, discoloration due to possible outgassing of a tether or cable material was again clearly visible on the Orbiter-facing EVA cargo transfer boom. Improved imagery of the Docking Module allowed additional characterization of discoloration of DM surfaces. Both the orange thermal blanket covering the DM and various hardware items attached to its surface exhibit some level of deposition/discoloration.

High resolution photography of the solar arrays, Kvant-2 radiator, and the Docking Module (DM) provides increased information on micrometeoroid and orbital debris (MMOD) strikes, and deposition/discoloration associated with the DM and elements attached thereto. Therefore, the surface assessment section focuses on the MMOD strikes and deposition/discoloration photography which was taken during the survey. The high resolution MMOD strike photography taken during this mission provides both coverage of newly-detected strikes and additional information on strikes which were identified on previous mission photography.

3.1 Micrometeoroid and Orbital Debris Damage Assessment

The high-resolution imagery acquired by the STS-84 crew provided details of MMOD strikes not previously available. In this mission report, the more distinctive strikes (in size and appearance) are shown and described. In addition, measurements and counts have been made for MMOD strikes in the regions surrounding the larger strikes. Results reported here are for three distinctively different Mir surface types: the thermal blanket of the Mir Docking Module, the painted metallic surface of the Kvant-2 radiator, and the solar cells of the Base Block, Kristall, and Kvant-2 solar arrays.

A comprehensive analysis of all imagery for MMOD strikes to the smallest size detectable is beyond the scope of this mission report. However, a separate database of MMOD strikes is being maintained. The data on the size and density of MMOD strikes is being used by NASA scientists and engineers in their development of the MMOD environmental models.

The structure and appearance of MMOD strikes are variable. However, Figure 3.1 is an illustration of a typical MMOD strike. The illustration is provided for purposes of description of the strikes.

The images on which MMOD strikes have been measured are high resolution and show only a small region. In order to estimate the sizes and damage of MMOD strikes, data from engineering drawings was used to scale the images. Intermediate images were used to translate dimensions from the drawings to a feature which exists in the image from which MMOD measurements were made. The reference features in the solar panels were individual solar cells. An unnamed feature was used for the Kvant-2 radiator. The feature used for the Docking Module was the distance between a pair of bolts.

The uncertainty in the MMOD measurements are primarily a function of the irregularity of the features that are measured (i.e., center pit and rings), scaling error associated with measurement of the cell boundaries, the obliquity of the image, and identification of the boundary pixels. The uncertainty, based on these sources, is estimated as approximately 10-15 percent (plus or minus) of the stated sizes of the strikes.

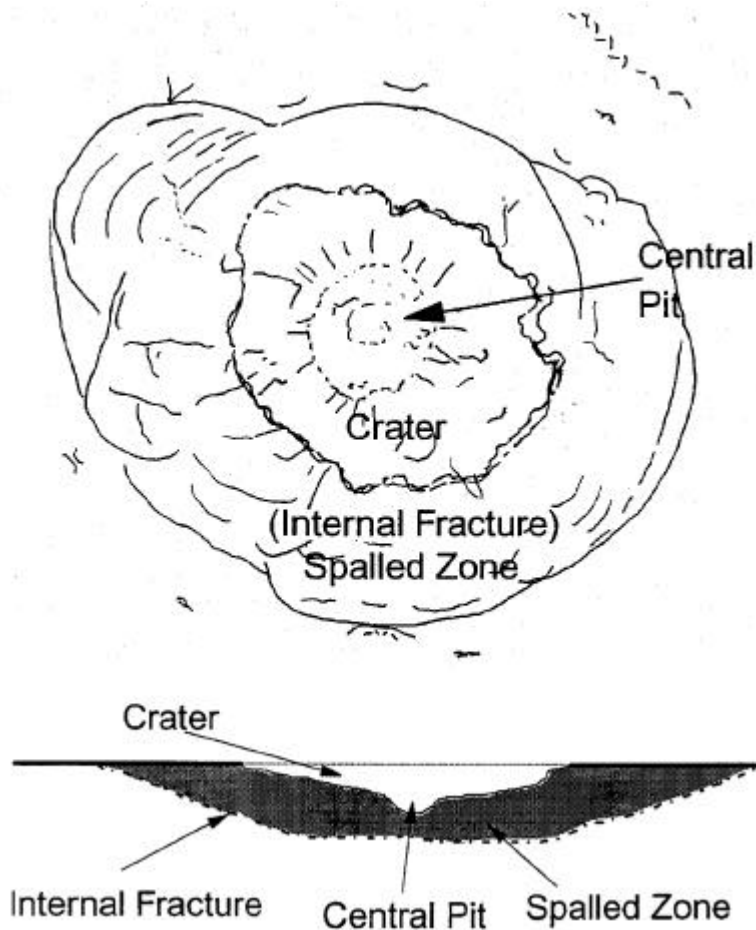


Figure 3.1 Typical View and Cross Section of MMOD Strike

Figure 3.2 shows three distinctively different MMOD strikes on Kristall SP#2. The strikes A, B, and C are located on the outer petal of the solar panel as shown by the arrow in the figure inset. The strikes have not been detected in previous mission imagery.

Strike A has a black center with two concentric outer rings and a fracture pattern extending over the dimensions of the solar cell. The black center indicates an apparent pit or hole of average diameter 3.0 mm. The first ring from the center has a dark brown appearance and an average outer diameter of 8.2 mm. This dark brown area may be a spall area of the back side of the silicon cell. A second, bright reflecting, ring of shattered glass extends to an average outer diameter of 13.4 mm. The extended fracture pattern of cracks in the outer glass extends out to the edges of the solar cell which are 2 to 4 cm from the edge of the “bright ring”. The measurements are based on scaling of the individual solar cells of dimensions 5.0 cm on a side.

The strike labeled B has an apparent penetration hole or crater of average diameter 1.8 mm and a surrounding bright area of average outer diameter of 9.2 mm. The bright area may be a spall area of fractured glass.

The strike labeled C has a strike average diameter of 2.4 mm. There is no apparent central pit or hole, indicating the strike may be limited to the cover glass.

A region of 7 by 7 cells (35 cm x 35 cm) surrounding the three strikes above was examined for additional MMOD strikes. Five additional strikes ranging in size from 1.4 mm to 3.5 mm were found.

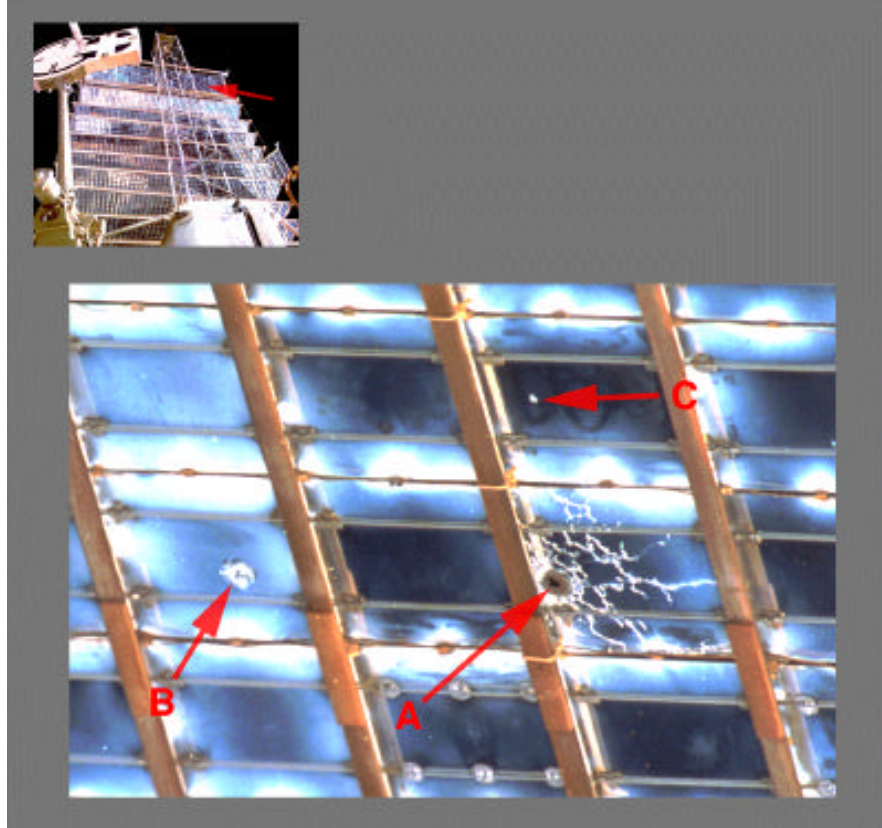


Figure 3.2 Kristall SP#2 MMOD Strikes

Base Block SP#2

Figure 3.3 shows MMOD strikes on Base Block SP#2 similar to those shown on Kristall SP#2. These strikes are located on the innermost of the two 387 cm wide petals of SP#2 as shown by the arrow in the inset image of Figure 3.3.

Strike A has a black center with two outer rings and a fracture pattern extending over the dimensions of a solar cell. The average diameter of the center black area is approximately 3.7 mm. The average outer diameter of the brown spall area is 6.6 mm and the average outer diameter of the bright area of shattered glass is 10.6 mm. The cracks extend to the boundary of the solar cell, which has been scaled from Mir drawing package measurements and images of the Base Block SP#2 to be 4 x 5 cm in size. The thin white lines within the cells are grid lines which collect electrical current generated by the cell. The wider horizontal white lines within the cells are ohmic bars which collect the current from the grid.

The small strikes B and C are measured to be 0.9 and 1.0 mm in size respectively. The uncertainty in the sizes of the strikes is approximately 10-15 percent (plus or minus) of the measured size of the strikes.

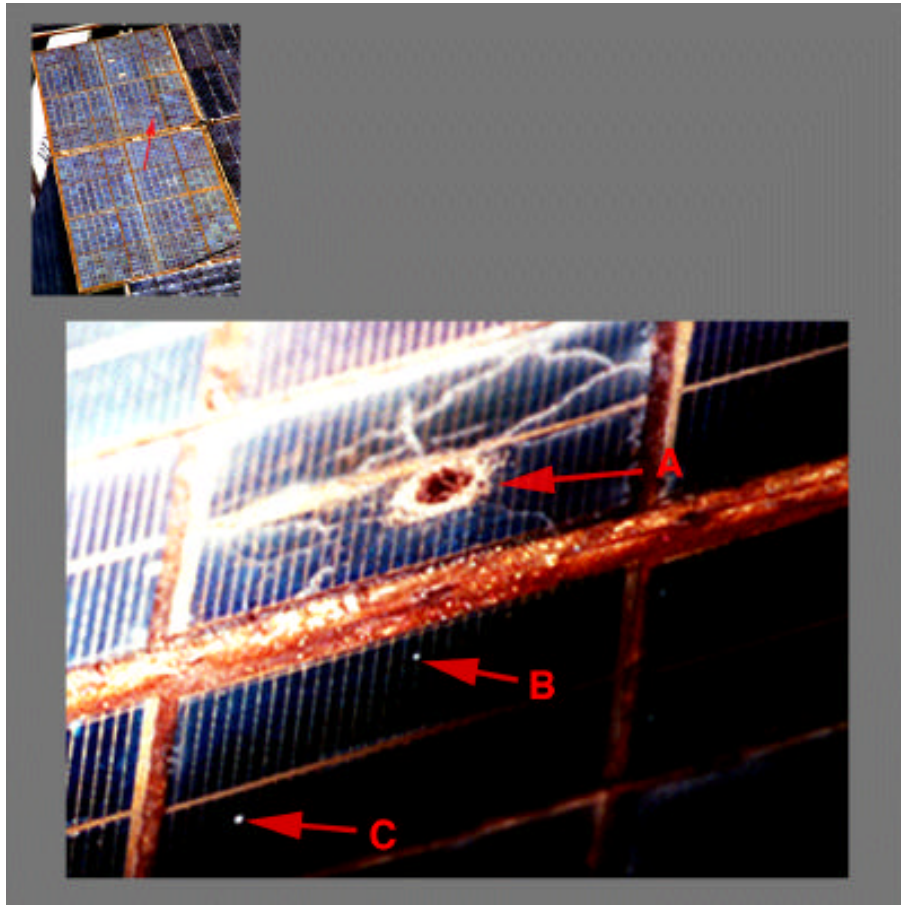


Figure 3.3 Base Block SP#2 MMOD Strikes

Figure 3.4 shows a circular MMOD strike on Base Block SP#2. The exact location of this strike on the Base Block #2 array has not been determined. However, the pattern of cells can be matched with areas of the Base Block SP#2 which appear to have cells of size 2 cm x 2 cm. According to information [Reference 7] by Dr. V. Khourunov of RSC-Energia provided to Thomas Kerslake, Lewis Research Center, Base Block SP#2 has both gallium arsenide and silicone cells of size 2 cm x 2 cm. It is not known which type of cell this is. The cell size boundaries were determined by multi-stage scaling from Mir drawing packages and imagery of varying scales collected on Shuttle/Mir flights starting with STS-63. On this basis, the dark central core of this strike is approximately 2 mm in diameter. Three rings extend outward from the central core. The first ring is a white area with an outer diameter of approximately 4 mm. This is apparently a spall area of shattered glass. The second ring is approximately 5 mm in diameter. This may also be a part of the spall area. The outer ring is approximately 8 mm in diameter. A count of 16 cells surrounding the strike in Figure 3.3 yielded five additional MMOD strikes in the size range 0.5 to 1.0 mm. Because the cell boundaries are difficult to identify for this image, the uncertainty of the measurements is greater here than in the previous strikes in

this report. The uncertainty is approximated to be on the order of 15-20 percent (plus or minus) of the measured strike size.

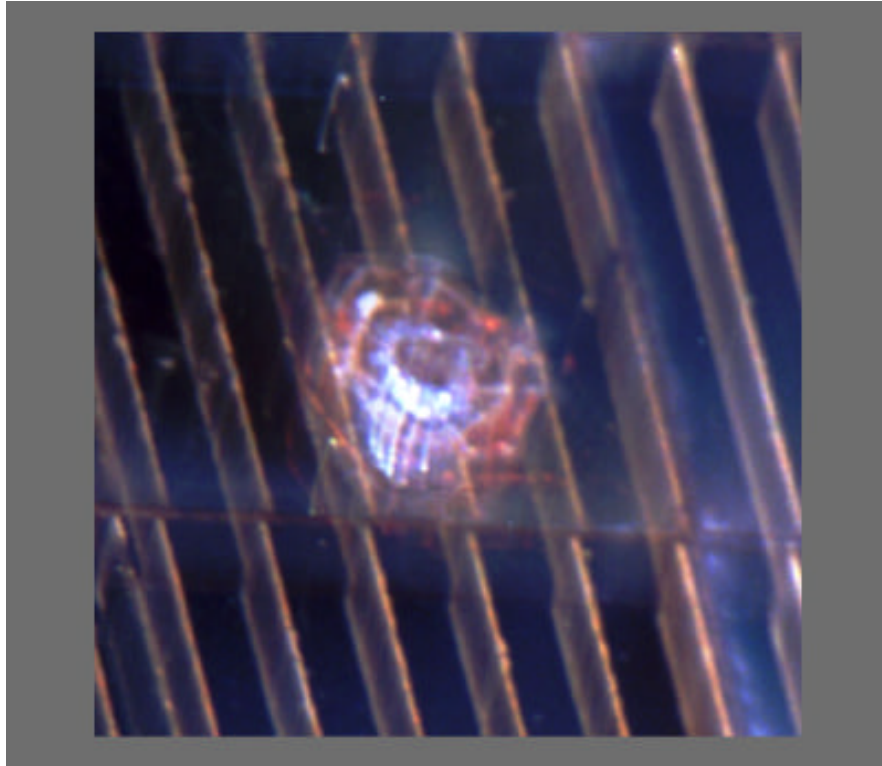


Figure 3.4 Circular MMOD Strike Pattern on Base Block SP#2

Kvant-2 SP#2

Figure 3.5 is a detailed view of a MMOD strike on the Kvant-2 SP#2. This strike was described in the STS-81 Mission Report [Reference 6], however the STS-84 image is of higher resolution and provides improved definitions of the central pit, spall zone, and cell dimensions. This strike is somewhat different from the strikes shown previously in that a radial pattern of rings does not exist. The damage area is also larger than those shown earlier. Each individual cell is 4 cm x 5 cm in size, and the damage extends over 4 of the cells. The structural component on the left of the image is along the center of the solar panel as shown in the inset to Figure 3.5. Note that the oblique view of the image distorts the aspect ratio of the sides of the cell. Compare to the back-side view (Figure 3.6) which is a nearly perpendicular view. The ohmic bars show in the front-side view but not in the back-side view.

The central black area is highly irregular in shape and extends 1.2 cm in the longitudinal (5 cm side) and transverse (4 cm side) directions of the cells. The adjacent white, semi-circular, area lacks definition and may be a specular reflection off an elevated rim. This white area is approximately 1 cm wide and extends 1.5 cm in the transverse direction. The brownish-colored area extends over all 4 cells and is splattered onto the adjacent

structural member. The total size of this brownish area is 7.3 cm x 7.5 cm in the longitudinal and transverse directions respectively. In addition, the splatter of the brownish substance appears to extend onto the edges of adjacent solar cells. The cover glass is possibly removed from one of the cells and portions of the other three cells. The cracks in the cover glass extend over the three cells.

It is not known whether the anomalous appearance of nearby cells is associated with the MMOD strike. A count of probable strikes over an area of 190 cells adjacent to the strike above yielded 19 strikes in the size range of 2.5 to 5.5 mm. The arrows in the figure point to some of the nearby MMOD strikes. The nearby strikes are not thought to be secondary strikes from the large debris strike because they are widely dispersed (in an area greater than 120° around the impact site). The uncertainty in the sizes of the strikes is estimated to be 10-15 percent of the size of the strike.

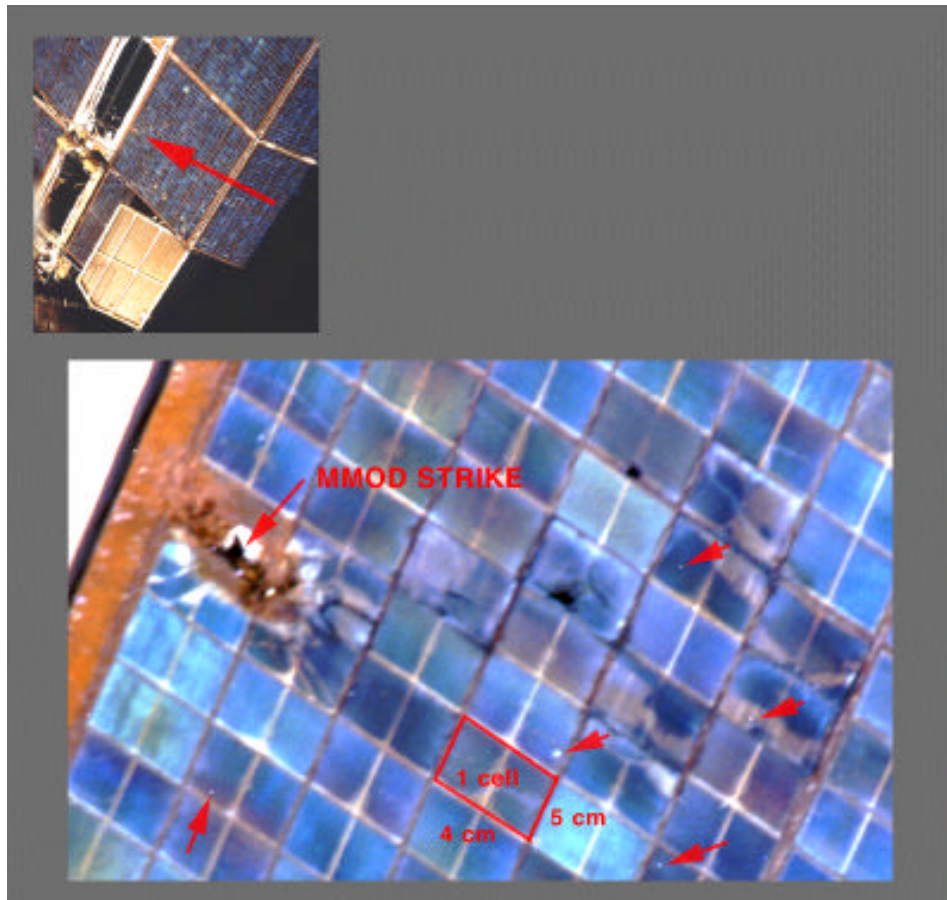


Figure 3.5 MMOD Strikes on Kvant-2 SP#2

Figure 3.6 shows the area of the debris strike on the backside of Kvant-2 SP#2 taken on STS-71. It is possible that the strike may have first impacted the backside of the solar arrays causing the damage observed on the front side shown in Figure 3.5. However, this has not been confirmed. The black central pit or hole has a similar shape on the back side as exists on the front side. The light colors are consistent in color with the back side of the solar cells and the supporting mesh. The light brown/yellow zone surrounding the dark central region corresponds to the regions where the cell cover glass has been removed on the front. The three nearby black areas correspond to cells which may be partially delaminated, but are not indicated as MMOD strikes. The larger rectangular grid in the image are the cell boundaries.



Figure 3.6 A View of the Back Side of Kvant-2 SP#2 MMOD Strike

Kvant-2 Radiator

Figure 3.7 is an extraction from a photograph which shows possible MMOD strikes on the radiator located on the -X, -Z side of Kvant-2 as shown in the inset image of Kvant-2. The larger strikes have an appearance similar to those shown on the solar arrays. They have a dark (black) central pit or hole surrounded with an apparent spalled zone where the white paint has been possibly removed. The larger strike has a central pit of approximately 10.9 mm in diameter and a spall zone of approximately 19.7 mm in diameter. Six additional possible debris strikes (denoted by arrows) are shown, with central pit diameters ranging from 3.3 to 5.5 mm in diameter. The other circular features on the radiator are rivets or round-head bolts, and can be identified by their highlights and shadows. The portion of the radiator shown in this figure is approximately 1630 sq cm in area. The possible strikes shown here are more uniform in diameter than the ones shown

previously. The uncertainty in their size is approximately 10 percent (plus or minus) of their measured size.

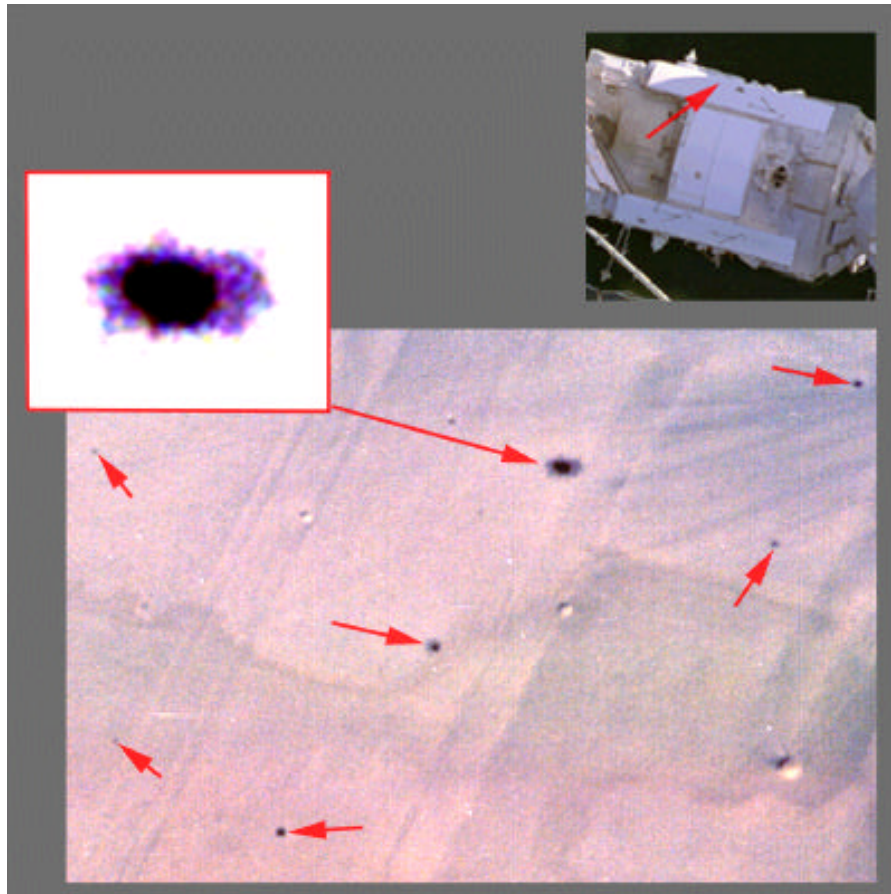


Figure 3.7 Possible MMOD Strikes on a Portion of Kvant-2 Radiator

Docking Module Thermal Blanket

Figure 3.8 shows six possible MMOD strikes in the Docking Module thermal blanket on the +XB side between the RSA and the OPM [1-5]. Inset 2 includes two strikes; the largest and the smallest strikes in the photograph. Each of these strike areas has a dark center surrounded by a white circular region. Outside this region is a much larger, dark circular region. Similar ringed features of MMOD strikes were observed on silver teflon thermal blankets and certain painted surfaces on the Long Duration Exposure Facility (LDEF) [Reference 8].

The largest strike has a dark center of 2.6 mm diameter, a white ring of 8.3 mm diameter, and a dark outer ring of 26.5 mm diameter. The smallest strike has a dark inner circle of 0.5 mm diameter, a white ring of 1.8 mm diameter, and a dark outer ring of 5.7 mm diameter. The surface area covered by the photograph is approximately 580 x 380 cm.

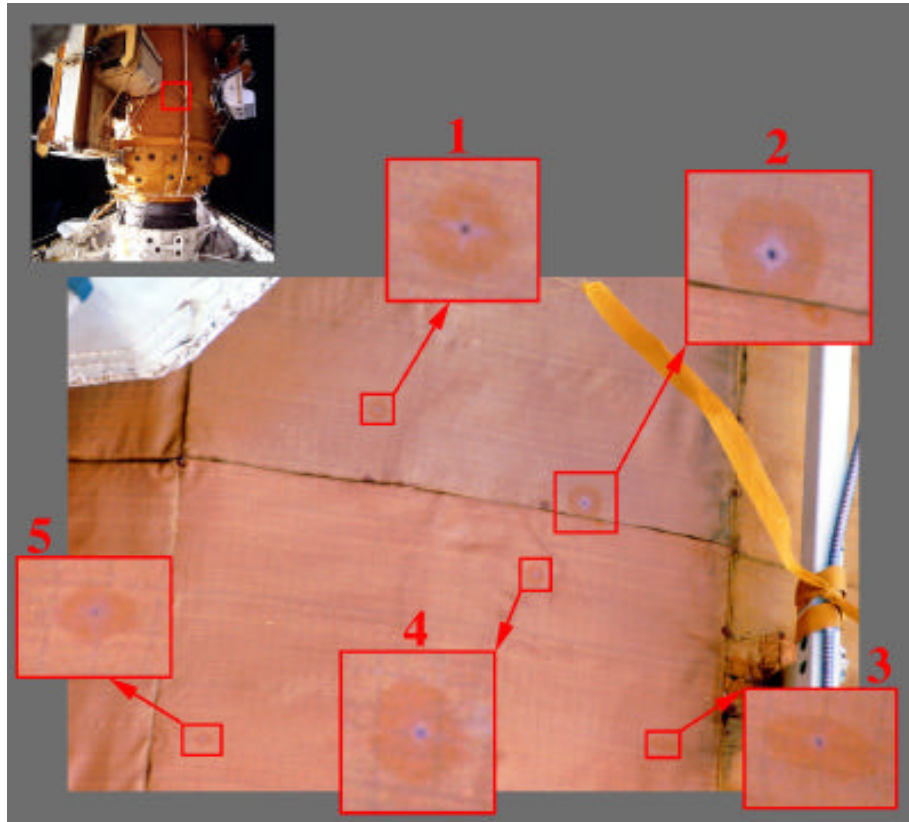


Figure 3.8 Possible MMOD strikes on Docking Module Thermal Blanket

Summary of STS-84 MMOD Results

Table 3-1 provides a summary of MMOD results from the STS-84 analyses. The results are tabulated according to the ranges of sizes of strikes measured. Where the strikes have a central pit or hole, those values are also provided. The spall sizes are also given. Note that not all strikes have identifiable central pits and not all strikes have identifiable spall zones. This effect is a function of the size of the strike and the type of Mir surface material where the strike occurred. All the central pits and spall zones are circular except for the strike on Kvant-2 SP#2. The central pit of this strike has an irregular shape and the spall zone includes one entire cell plus portions of three other cells. It can not be determined how much of the cells may be removed by the strike.

The process for identifying, locating, and measuring the MMOD strikes has been somewhat tedious and time-consuming, especially for the strikes on the solar panels. The high-resolution images, from which the larger strikes can be described and the smaller strikes identified, cover only a small portion of the solar panel. The pattern of cells is the primary feature for determining the location of the image. However, the pattern of cells is duplicated over many areas of the solar panel. Intermediate images of lower resolution are of primary value in locating the image and the strike locations. The STS-63, STS-71,

STS-74, and STS-81 images were used in determining the locations and sizes of cells in the region of the strikes.

The strikes listed in the table have been identified and measured with a high degree of reliability. However, there are smaller strikes than those in the table that are visible in the STS-84 photographs that have not been measured or counted. The reason for this is that counts of smaller strikes are subject to variations in image quality within a single photograph. Reliable analyses for smaller strikes need to have, and utilize, multiple photographs. This will involve overlapping photography within a single mission, imagery from multiple missions, and take full advantage of the bracketed exposures of the photographs. It will also require a significant additional workload, not only in the analysis, but in the enlargement and digitization of duplicate film masters from the missions.

The dimensions of the solar cells are best features for measuring the size of strikes on the solar panels. However, the cells vary significantly in size both within and between solar panels. Therefore, detailed analyses were required to determine the cell sizes for the specific local region of the strikes to establish the scale of the image and measure the size of the strikes and their features. The locations and accuracies of the strike measurements are provided in the preceding text.

The 10.9 mm strike on the Kvant-2 radiator has the characteristic appearance of a strike, but is anomalously large relative to all the other strikes. It is also curiously similar in size to strikes estimated at 10 mm size in the STS-71 imagery of a different Kvant-2 radiator. The existence of two strikes of this size in the same vicinity should be evaluated by the MMOD modelers.

The results in Table 3-1 were derived from an analysis of only six high-resolution photographs from STS-84. The six photographs are a small percentage of the approximately 1000 photographs of Mir surfaces which were taken on STS-84, including 400 photographs of solar panels. Many of these photos are duplicates and others may not be of sufficient resolution to reliably identify MMOD strikes. However, there are additional images which can be used for MMOD strike identification and measurements.

Table 3-1 Size Distribution of MMOD Strikes from STS-84 Images

Region	Size of Area Analyzed (sq cm)	# Strikes by Size Distribution	Diameter of Central Pit (mm)	Diameter of Spall (mm)	Comments
Kristall SP#2	1225	1 5	3.0 -	8.2 1.4 - 3.5	5 x 5 cm cell fractured
Base Block SP#2	40	1 2	3.7 -	6.6 0.9-1.0	4 x 5 cm cell fractured
Base Block SP#2	65	1 5	2.2 -	5.2 0.6-0.9	2 x 2 cm cell size
Kvant-2 SP#2	3800	1 19	120 -	- 2.5-5.5	Spall size of 30 sq cm
Kvant-2 Radiator	1630	1 6	10.9 3.3-5.5	19.7 -	
Docking Module	220400	6	0.5-2.6	-	

3.2 Surface Deposition and Discoloration

Imagery taken of Mir starting with STS-63 (February 1995) has revealed deposition/discoloration on all Mir modules and has been documented in all previous mission reports. The deposition/discoloration portion of this report focuses on the Docking Module (DM) surfaces which were photographed in detail during the STS-84 mission. New details of deposition/discoloration are observed in the photographs of the DM thermal blanket, Reusable Solar Array (RSA) carrier, Remotely Operated Electrical Umbilical (ROEU) Payload Disconnect Assembly (PDA), and the Optical Properties Monitor (OPM). In addition, the area of discoloration (stain) of a possible leak in the Spektr radiator is compared to STS-81 mission imagery.

Reusable Solar Array

Figure 3.9 is the highest resolution photograph to date of the base of the RSA which faces the Shuttle during the docked phase. Photography from previous missions showed deposition on this surface. However, higher resolution and improved lighting reveal the consistency in deposition across the outer plate of the corner [1], which was originally white. Inner edges [2] of holes cut out of the plate do not appear to have received as much deposition as the outer surfaces.

Figure 3.10 is a photograph of the surface of an RSA Carrier Hinge which appears to have some surface anomaly, possibly a scratch [1]. This area is white in color, and this may be due to the surface being more reflective than the surrounding area which is gray in color. This scratch has not been seen previously. In addition, there are some brown areas of discoloration which were also visible in photography from STS-76 [2].

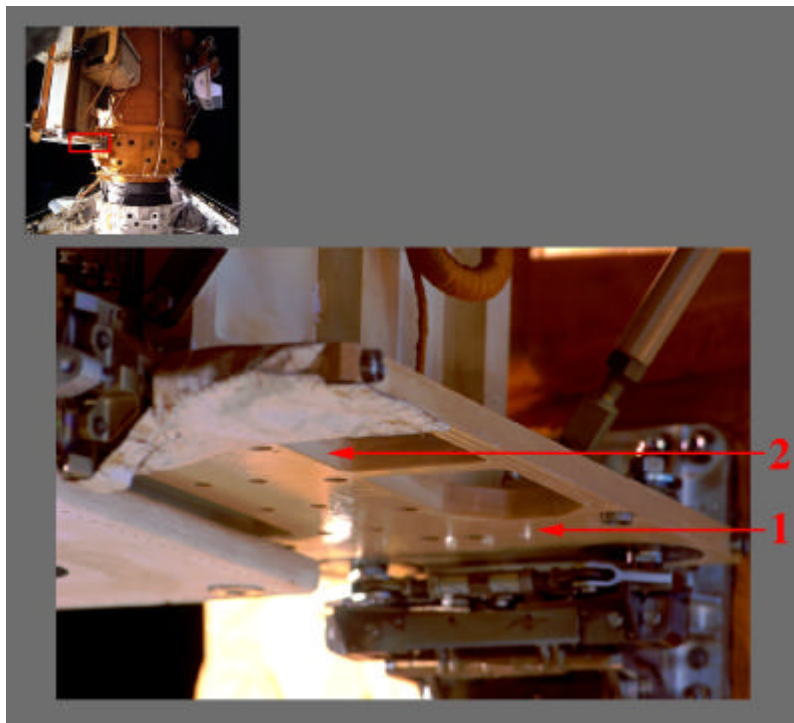


Figure 3.9 Deposition on Base of RSA Carrier

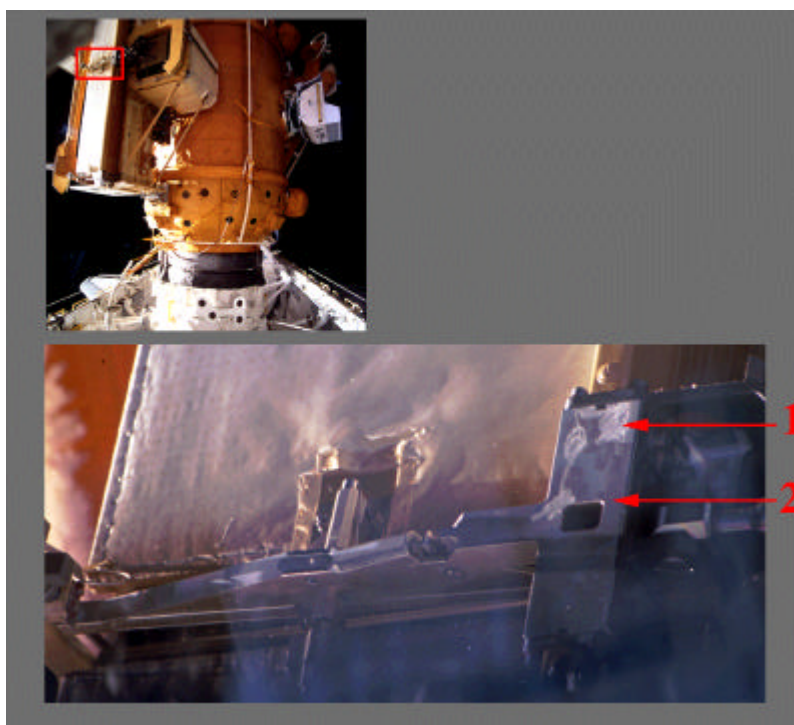


Figure 3.10 Irregularity on Surface of an RSA Carrier Hinge

Docking Module Thermal Blanket

Figure 3.11 is a photograph of the thermal blanket on the Docking Module. There is a region of the blanket which has an uneven dark discoloration [1]. There is a circular stain which suggests that a contaminant may have permeated the surface or leached through from underneath the surface [2]. The photographs taken during this mission are the highest resolution to date of the thermal blanket.

ROEU Payload Disconnect Assembly

Figure 3.12 is a photograph of a large area of dark deposition on at least one of the four prongs on the Remotely Operated Electrical Umbilical (ROEU) Payload Disconnect Assembly (PDA) [1]. A small region of this same prong [2] appears to have received little deposition since it remains white in color. This preferential pattern of discoloration may suggest that the trajectory of the contaminant causing this deposition remains relatively constant. The JSC Cargo Engineering Office is concerned that deposition on the surface of the connectors could cause uneven thermal cycling, thereby reducing the lifetime of the connector.

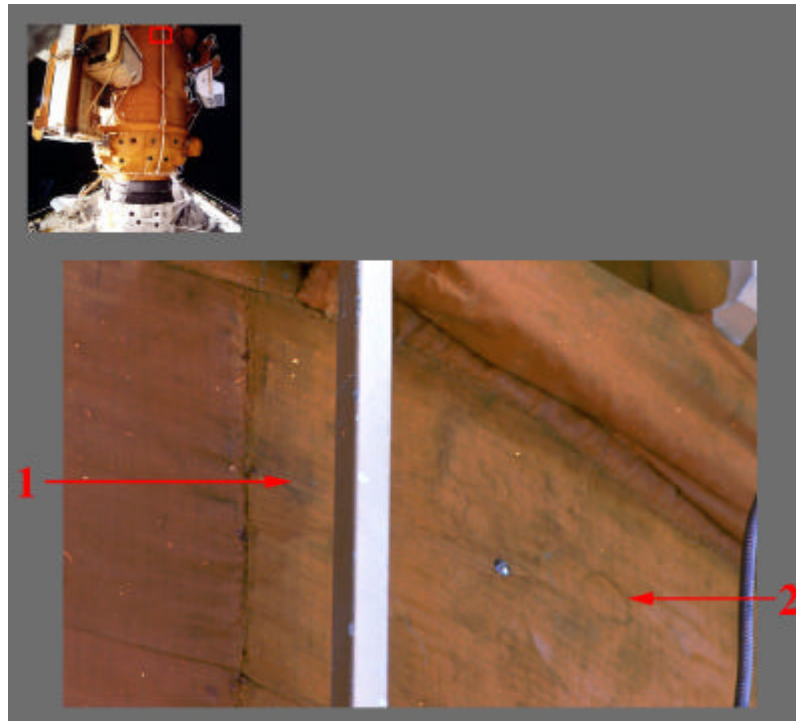


Figure 3.11 Discoloration and Possible Stain on Docking Module Thermal Blanket

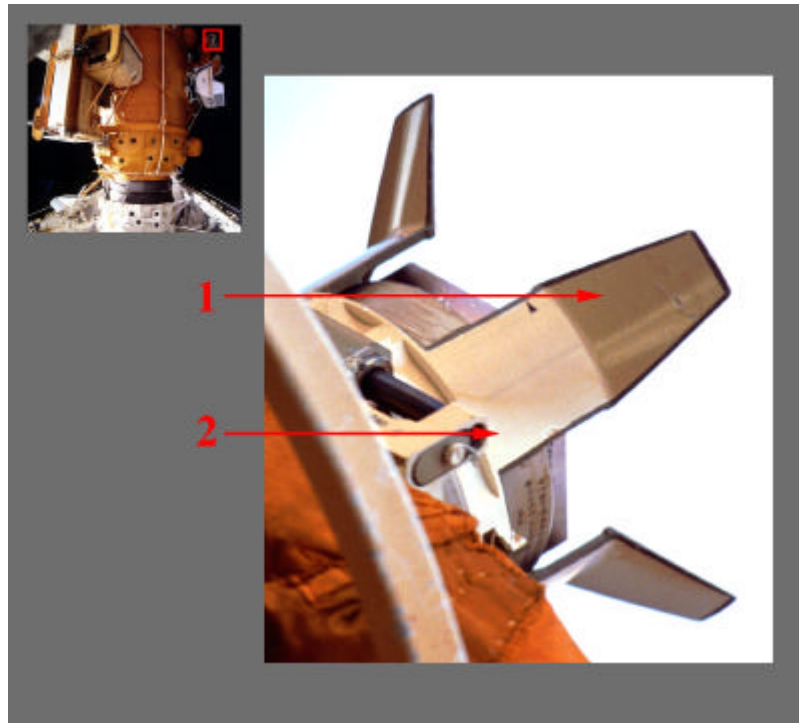


Figure 3.12 Docking Module - ROEU-PDA

Optical Properties Monitor

Figure 3.13 is a photograph of the OPM which was deployed on the Docking Module during an EVA on April 29, 1997. This photograph, taken around May 20, 1997, reveals deposition on a thermal blanket covering the end of the OPM facing the (+XB) direction. There is a highly preferential pattern of discoloration on this thermal blanket. There are areas to the left of the handrail and Mir crane interface in this picture that appear to be receiving little deposition [1, 2 respectively]. These objects protruding from the surface appear to block the deposition which is striking the rest of the thermal blanket, creating a “shadow” of these items to the left of the actual object. The direction the contamination is originating from appears constant enough for even the thinnest object, in this case a wire attached to the handrail, to cast a “shadow” [3].

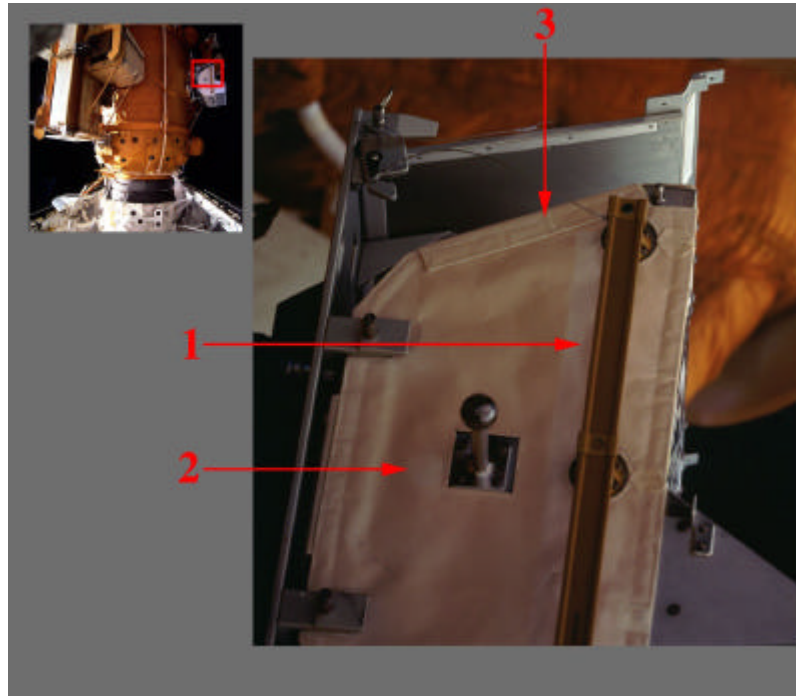


Figure 3.13 Docking Module - OPM

Spektr Radiator

Figure 3.14 shows the progression of a possible leak on the Spektr radiator. This possible leak was first identified on the STS-81 Mir survey imagery. This leak appeared as an orange-colored stain on the radiator. A review of previous mission imagery showed the leak originated between the STS-74 and STS-76 missions. However a significant increase in size occurred between the STS-79 and STS-81 missions. The progression of the leak from STS-79 to STS-84 is shown in Figure 3.14. There were additional increases in the area of the leak as shown by the arrows in the STS-84 image. However, the increases were small and did not show the dramatic increase in area that was observed in the STS-81 imagery. The size of the leak remained at approximately 7 sq cm.

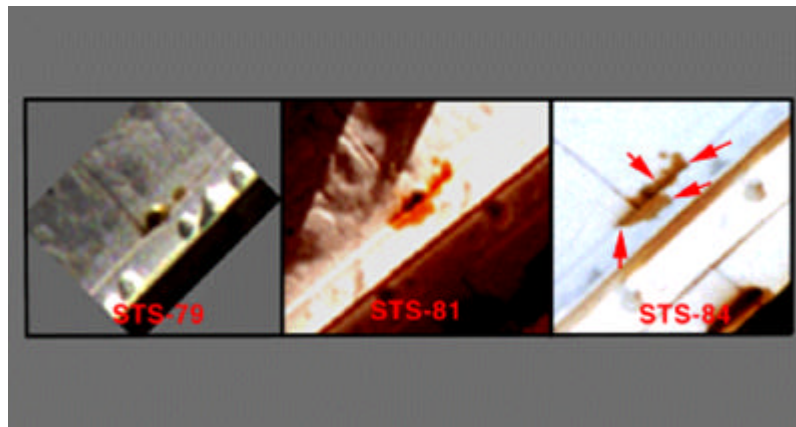


Figure 3.14 Progress of Possible Leak on Spektr Radiator

4. DOCKING MECHANISM ASSESSMENT

Imagery of the docking mechanism obtained on STS-84 was examined to verify its condition in preparation for STS-86. The imagery included both film photography and video acquired during approach and backaway. Close-up film photography of the docking mechanism was not obtained during either approach or backaway.

Docking occurred during darkness for STS-84. The video imagery obtained with the ODS centerline camera during approach showed the docking target to be in good condition. However, there were significant reflections in the video when the docking latches were in the field-of-view and the video was focused on the docking target. The video imagery was not suitable for assessment of the docking latches, alignment guides, electrical connectors, or retroreflectors. However a view taken with the 35 mm camera and telephoto lens during approach was sufficient to show the capture and structural latches were in proper position and the centerline and non-axial targets in good condition. The retroreflectors and electrical connectors appear to be in good physical condition, however, the imagery was not of sufficient resolution to detect discolorations that might exist. The image is shown in Figure 4.1.

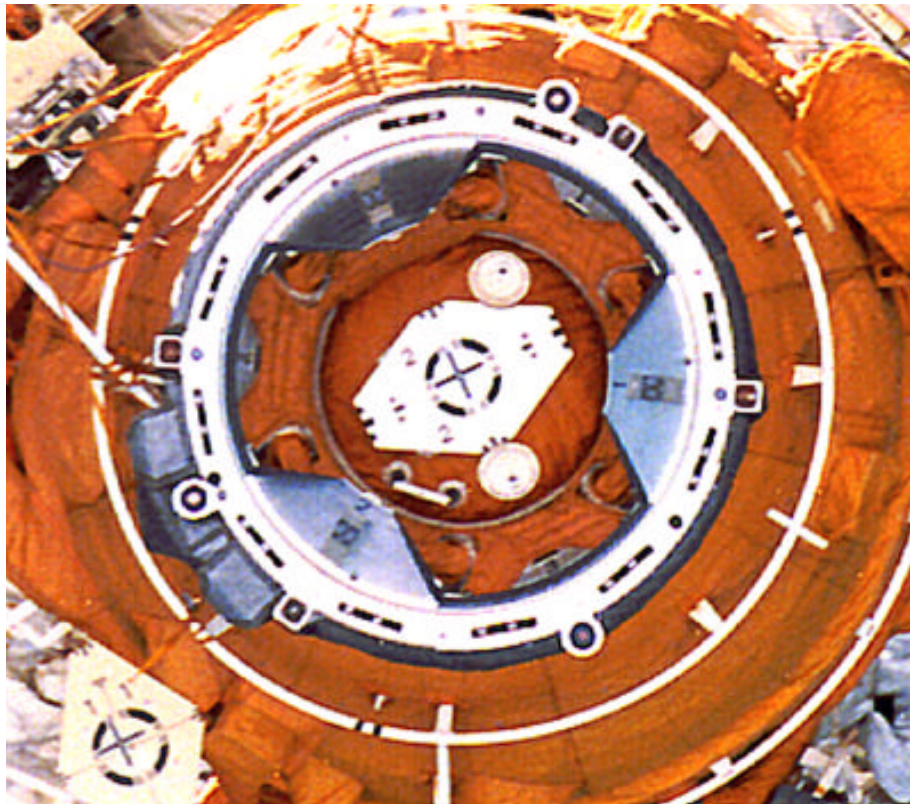


Figure 4.1 Photo of Docking Mechanism during Approach

Undocking and backaway also occurred during darkness. During backaway, however, the centerline video camera was set to a larger field-of-view than for docking, and video was obtained of the docking mechanism without the reflections observed during

approach. This video shows the capture and structural latches to be in the proper position and the docking target to be in good condition. The electrical connectors and retroreflectors appear to be in good physical condition, however the video is not sufficient to detect significant discolorations. The video image is shown in Figure 4.2.

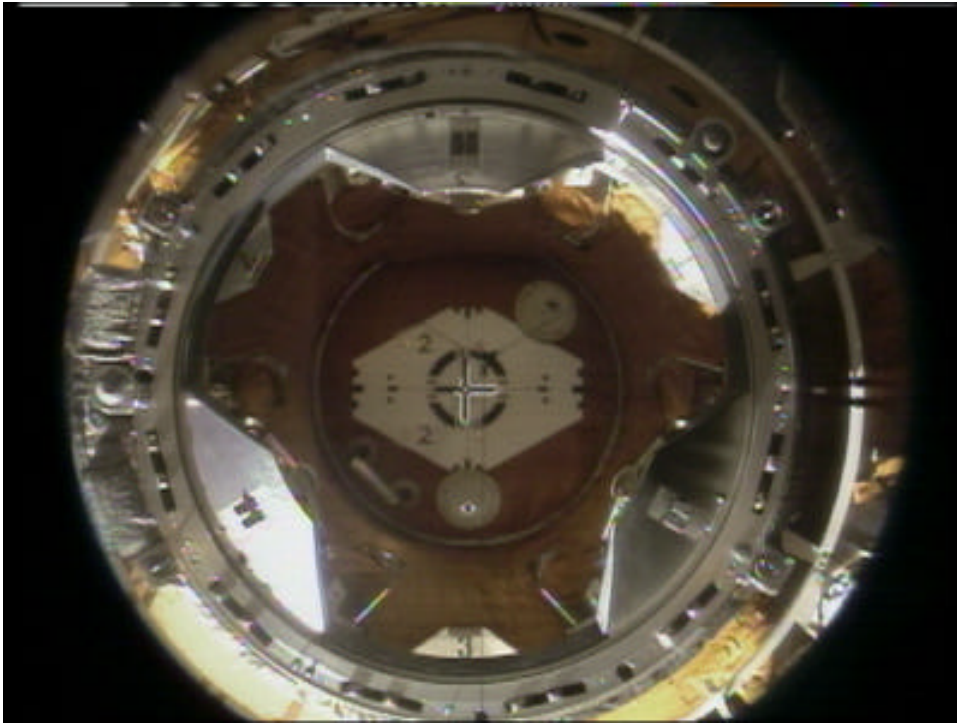


Figure 4.2 Video of Docking Mechanism during Backaway

5. MIR STRUCTURAL DYNAMICS EXPERIMENT SOLAR ARRAY MOTION

Image analyses of the motion of Mir solar arrays have been performed since the first Shuttle docking flight to Mir, STS-71. Frequency and amplitude measurements from imagery have been made for the Kvant SP#1, Kvant-2 SP#2, Base Block SP#2, Spektr SP#2, and the Cooperative Solar Array (CSA). During STS-71, STS-74, and STS-81, tests were conducted with the firing of Shuttle Reaction Control System (RCS) thrusters while the Shuttle was docked, and the amplitude and frequency of solar array motion was recorded and measured. Measurements have been correlated to the Shuttle thruster firing times through the use of timing on the video. These data on solar array motion were provided to the JSC Structures and Mechanics Division for use in structural dynamics modal analyses and support to International Space Station (ISS) loads verification.

The Mir Structural Dynamics Experiment (MiSDE) is a risk mitigation experiment for the ISS. The purpose of the experiment is to obtain dynamic structural response data on the Mir. Accelerometers are placed throughout the Mir and measure accelerations in three dimensions as the Mir responds to a variety of dynamic load stimuli. Crew exercise activities on-board the Mir and timed thruster firings from the Shuttle and Mir are the most notable sources of perturbation. In addition to the accelerometers, video of solar array motion is captured during the timed thruster firings for correlation with the accelerometer response.

5.1 Solar Array Video Data Acquisition

During STS-84, video data of the motion of Base Block SP#2 during four controlled thruster firing sequences from the Shuttle was acquired. A table of the firings is shown in Table 5.1. Only test sequence #2 provided a detectable motion in the video. One minute of Sequence #2 was selected for analysis of the array motion. This sequence of video was selected to encompass a time span prior to, during, and after the Mir thruster firing sequence based on the IRIG timing on the tape. A multiplexed video frame used in the analysis of the Base Block SP#2 motion is shown in Figure 5.1. The tracked point is labeled in the figure with an arrow.

Simultaneous sequences of video frames from two cameras were acquired to obtain the three-dimensional motion of a point on the array. Video at both the array tip and the array attach point at the module allowed the measurement of module motion to be removed from the measurements of the motion of the array tip. During the Shuttle thruster firings, payload bay cameras A and D recorded motion at the tip of Base Block SP#2, while cameras B and C recorded motion at the array attach point. As was the case with the STS-81 MiSDE data, motion at the array attach was too small to be reliably measured from the video data.

Once each camera acquired the array, camera pan and tilt settings were fixed for the duration of the thruster firing sequence. At the conclusion of the sequence, the camera views were demultiplexed. Each camera's pan and tilt was then adjusted to acquire video of the Docking Module. The zoom of the camera was held constant during this procedure

so that features of known size on the Docking Module could be used to establish the camera scale parameter in the data analysis.

Table 5-1 Shuttle Thruster Firing Sequences for MiSDE

Test Number	Jet Command	RCS Jet ID	Jet on Time (GMT)	Jet off Time (GMT)	Duration (sec)
1	+Y	F5L, L5D, R5D	140:06:24:18.787	140:06:24:23.827	5.040
	-Y	F5R, L5D, R5D	140:06:24:24.787	140:06:24:29.827	5.040
	+Y	F5L, L5D, R5D	140:06:24:30.707	140:06:24:35.747	5.040
2	-Y	F5R, L5L	140:06:27:27.427	140:06:27:29.427	2.000
	+Y	F5L, R5R	140:06:27:29.667	140:06:27:31.667	2.000
	-Y	F5R, L5L	140:06:27:31.747	140:06:27:33.747	2.000
	+Y	F5L, R5R	140:06:27:33.907	140:06:27:35.907	2.000
3	+P	F5L, F5R	140:06:30:29.187	140:06:30:32.227	3.040
	-P	L5D, R5D	140:06:30:32.227	140:06:30:35.187	2.960
	+P	F5L, F5R	140:06:30:35.187	140:06:30:38.147	2.960
	-P	L5D, R5D	140:06:30:38.227	140:06:30:41.267	3.040
4	-R	F5L, L5L, R5D	140:06:33:34.947	140:06:33:38.867	3.920
	+R	F5R, L5L, R5R	140:06:33:38.867	140:06:33:42.787	3.920
	-R	F5L, L5L, R5D	140:06:33:43.027	140:06:33:47.027	4.000

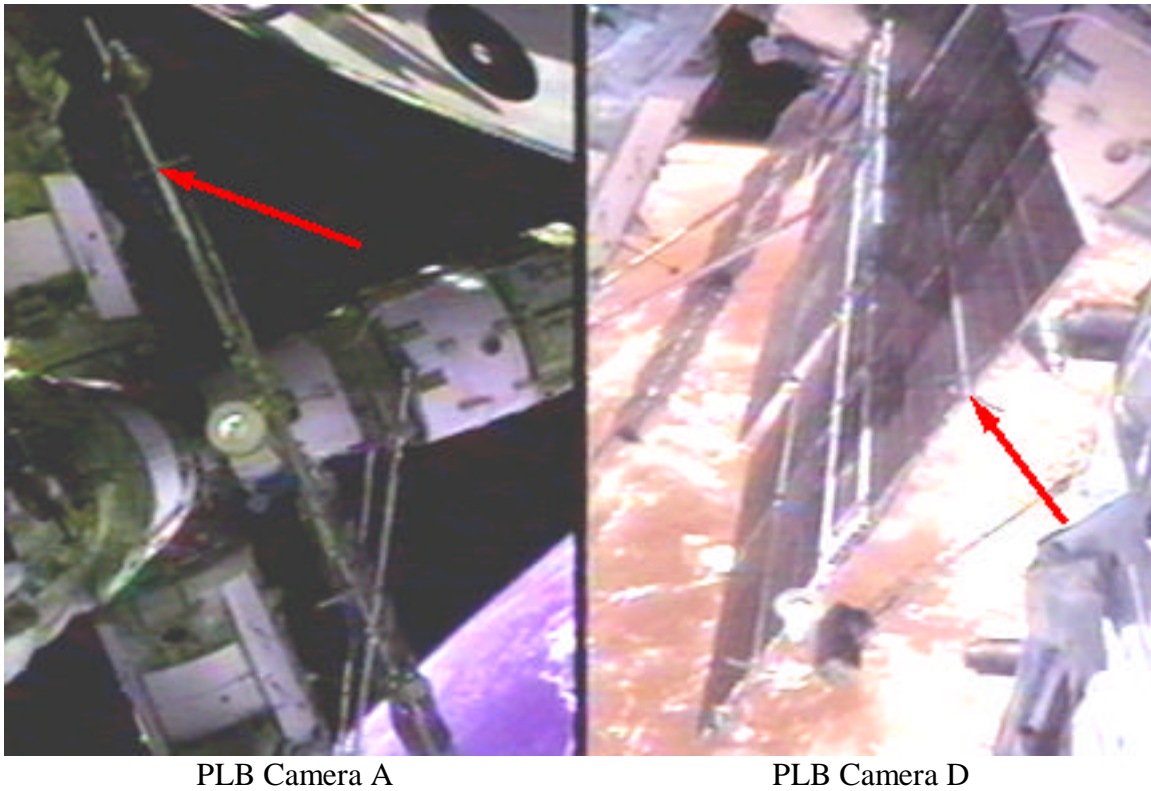


Figure 5.1 A Multiplexed Video Frame Used in the Motion Analysis of Base Block SP#2

5.2 Data Analysis Approach

The STS-84 motion analysis of the recorded video of Base Block SP#2 utilized a new software program which provided improved tracking of a point in a video sequence. The point tracking software allows the user to select a point to be tracked, a region of interest containing that point (to reduce computation time compared to a full frame of video), and a computational area of user-defined size. This computational area is compared to areas of the same size in the region of interest using a normalized cross-correlation function. To improve the accuracy of the program into the sub-pixel range, a cubic interpolation of the data is performed. Once the correlation between two frames is determined, a region of the same size as the computational area is located in the correlation data. This interpolation area is centered about the maximum of the correlation data. A cubic function is then “fit” to the interpolation area. Typical divisions of a pixel for interpolation subdivide it into 1,000 to 10,000 smaller “sub-pixels.” The maximum of this interpolation region represents the point to be tracked, i.e., the location of highest interpolated correlation. This X and Y position data in image coordinates, as well as a measure of the correlation between each of the frames, is saved to a data file.

An in-house software package utilizing standard photogrammetric techniques is then used to determine the location of the point in Shuttle coordinates. Several data inputs are required for the photogrammetry software. These include the image coordinates of the point being tracked for each frame, the image coordinates and object space coordinates of control points, and the object space coordinates of the cameras. The coordinates of known points on the Docking Module were used for determination of the orientation angles (pointing directions) and effective focal lengths of the cameras. The photogrammetry software computed, for each video frame, the Shuttle coordinates for the point being tracked.

A three-dimensional transformation was made from Shuttle to Mir coordinates to describe in-plane and out-of-plane array motion with respect to the Mir body coordinates. The results of the Base Block SP#2 motion analyses were then transmitted to the MiSDE principal investigator for structural dynamics analyses.

5.3 Results

The results from the motion analyses are shown in Figures 5.2 and 5.3 for the out-of-plane and in-plane motions as a function of time. Thruster firings are noted with black arrows. To reduce the effect of high frequency noise in the measurements of the deflection of the solar panel, a moving average over 15 frames of the deflection data was calculated starting approximately 25 seconds before the first thruster firing to approximately 25 seconds after the last thruster firing. The peak-to-peak deflections were approximated from these smoothed curves as 0.14 ± 0.10 inches for out-of-plane motion and 0.27 ± 0.07 inches for in-plane motion. These results are representative of the thruster firings which are in the yaw direction, which would be expected to create larger motion in-plane relative to out-of-plane motion. In addition, the small magnitude of deflection was consistent with the visual examination of the video which showed only a barely perceptible motion when the video was played at three times normal speed.

The standard deviation, σ , of the peak-to-peak deflection was calculated as $\sqrt{2} \sigma_s$, where σ_s is the standard deviation of the deflection values from the smoothed curve. This value was calculated over one cycle centered about the peak-to-peak deflection. These values are 0.10 for the out-of-plane motion and 0.07 for the in-plane motion.

It should be noted that these error values are applicable to this data set only and may not reflect the error associated with other data sets taken from an identical experimental setup and procedure. This is due to parameters that are not static from mission to mission (crew movement, array heating, etc.).

A Fast Fourier Transform (FFT) was applied to determine the dominant frequency. The graphs of the FFT's for the out-of-plane and in-plane data are shown in Figures 5.4 and 5.5. To emphasize the frequency of the motion and remove the frequency data associated with the sampling rate of the data, a small section of the Fourier transformed data is plotted. The dominant frequency for the in-plane motion is approximately 0.24 Hz and approximately 0.27 Hz for the out-of-plane motion.

The analysis of the small amplitude (0.27 inches) motion from the STS-84 data set was enhanced by the following:

- The Base Block array was approximately 11 feet above payload bay camera A. At this distance the pixel resolution is approximately 0.3 inch/pixel. Narrowing the field of view, decreasing the camera to object distance, or both would further improve the minimum resolvable amplitude.
- The video processing facility was reconfigured to allow direct digital transfer of images from video tape to computer. This deleted an analog-to-digital conversion step which was a major source of video noise.
- The sub-pixel technique described in section 5.2 allowed amplitudes to be measured that would have been impossible to determine if the data were processed at the pixel level.

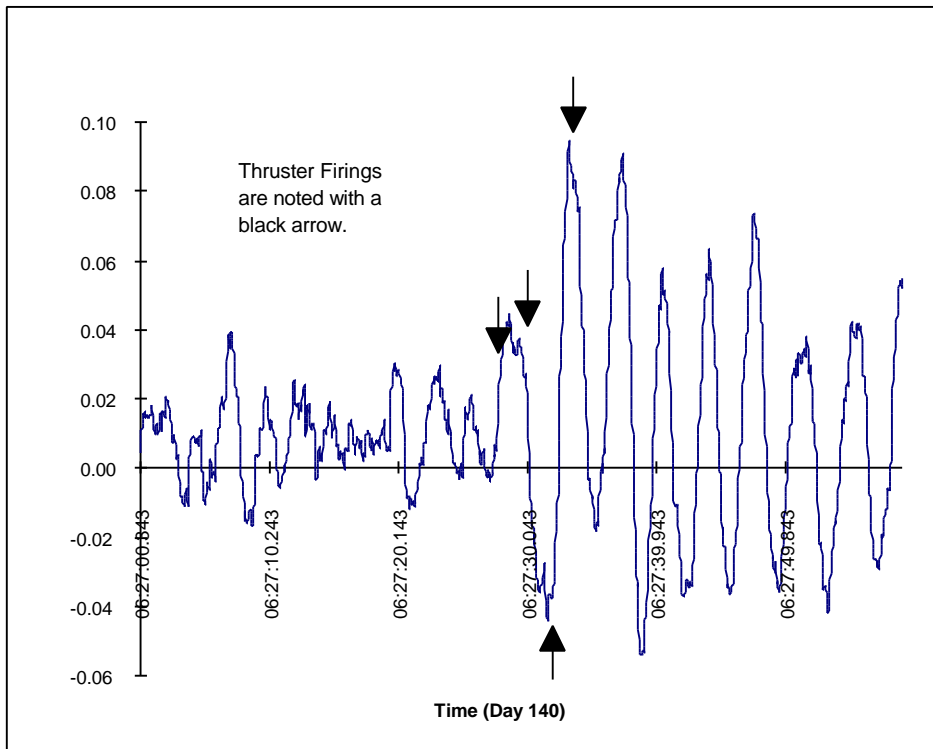


Figure 5.2 Out-of-Plane Deflection of Base Block SP#2

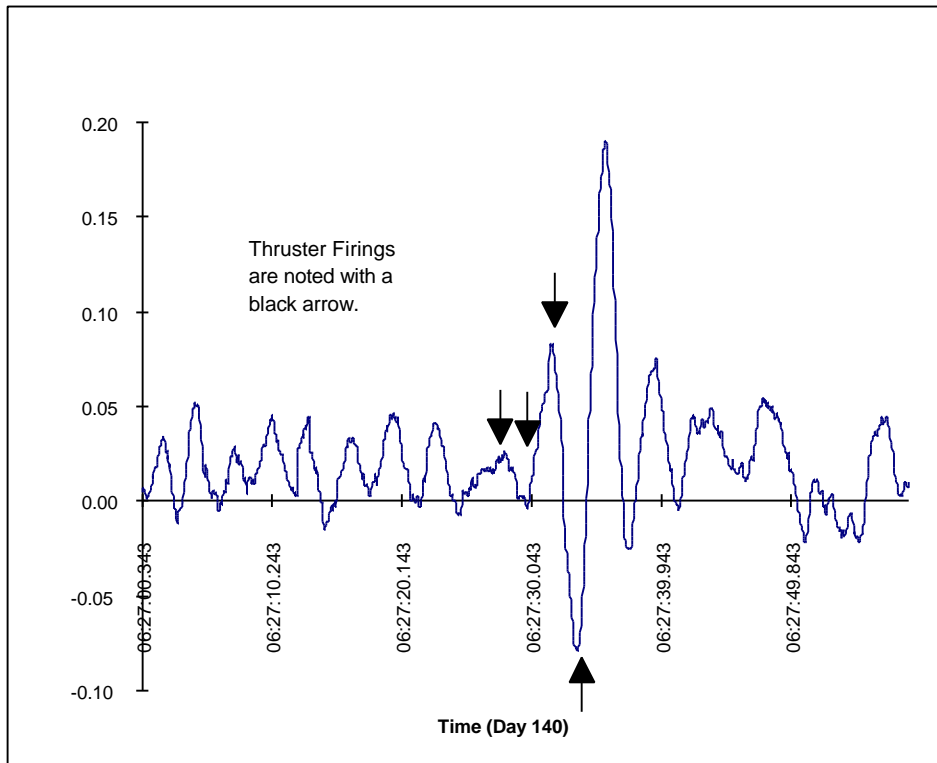


Figure 5.3 In-Plane Deflection of Base Block SP#2

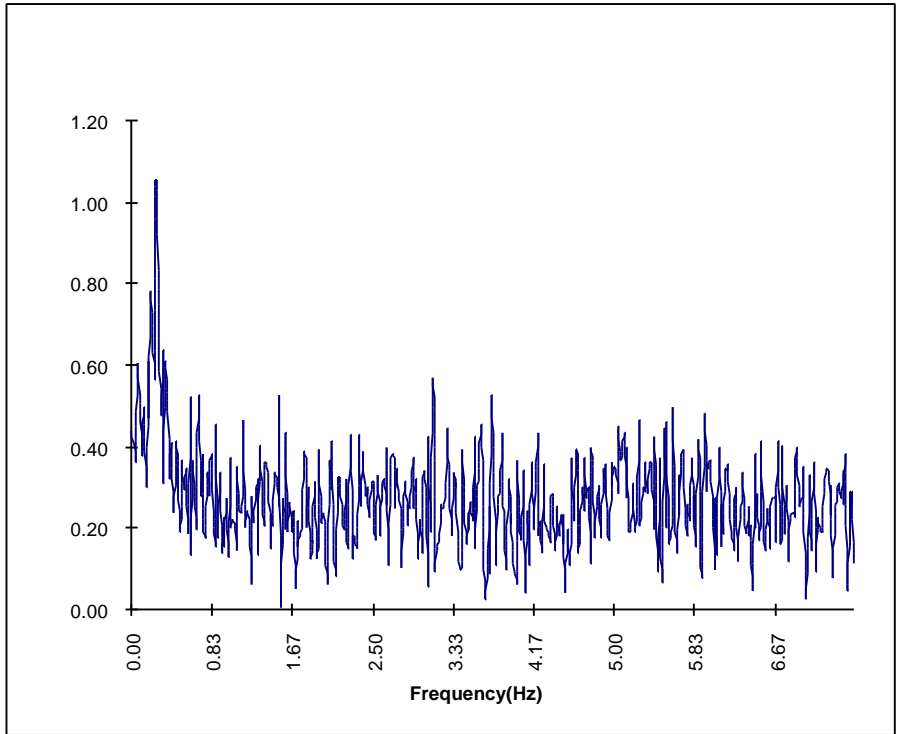


Figure 5.4 Out-of-Plane Frequency of Base Block SP#2

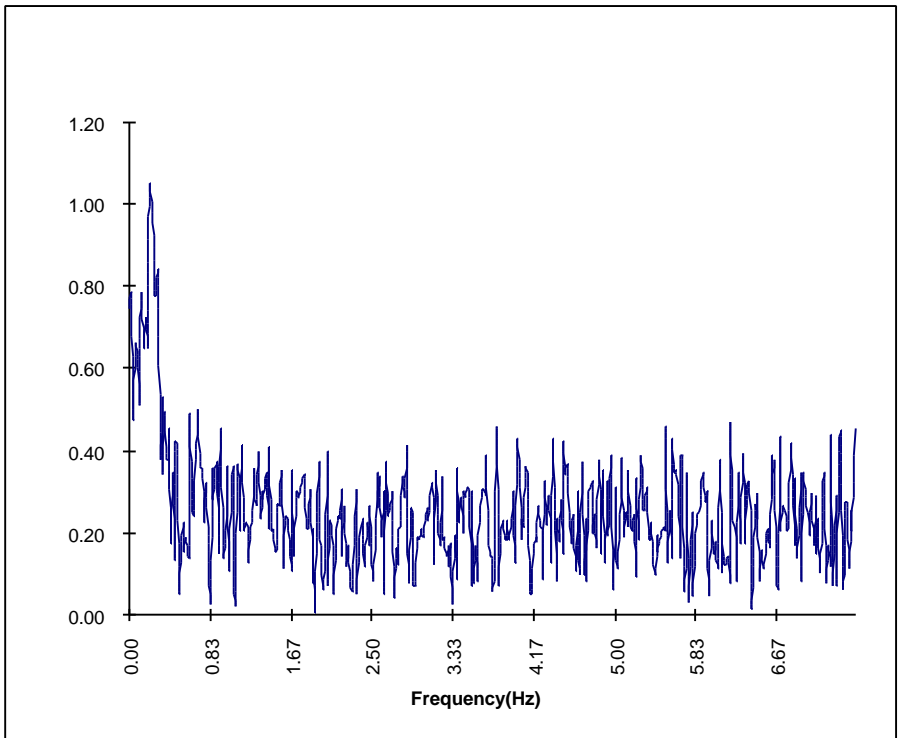


Figure 5.5 In-Plane Frequency of Base Block SP#2

6. DEBRIS DURING DOCKING OPERATIONS

Small pieces of debris are normally seen on orbit during most Shuttle missions. The previous Shuttle missions to Mir have shown extensive debris emanating from the area of interface of the Mir Docking Module (DM) and the Shuttle Orbiter Docking System (ODS) just after first contact was made and simultaneous sunrise occurred. Similar debris was not observed in the STS-84 video because docking occurred prior to sunrise. Sunrise provides background illumination which facilitates visibility of small debris. Most small debris is believed to be paint flakes or ice.

The ODS centerline television camera (CTVC) also did not show small debris within the ODS at the time of docking. The previous two Shuttle/Mir missions, STS-79 and STS-81, showed debris specifically originating from within the ODS, and was recorded by the CTVC.

However, three minutes and thirty-one seconds after docking contact, a single piece of debris was observed moving vertically in the Shuttle +Z direction in the line-of-sight between PLB camera A and the Docking Module. This piece of debris and its path are shown in Figure 6.1. The debris is observed to make contact with the thermal blanket on the lower side of the Reusable Solar Array (RSA) carrier, deflect several times and continue on its +Z path. The exact shape of the debris cannot be determined, but appears to be a polyhedron as shown in the inset in Figure 6.1. Because the debris makes contact with the RSA carrier, it is possible to make an estimate of the velocity of the debris by scaling its distance with the adjacent DM dimensions. Prior to making contact the +Z velocity is approximately 25.4 cm/sec. Its +Z velocity after making contact and continuing on its new

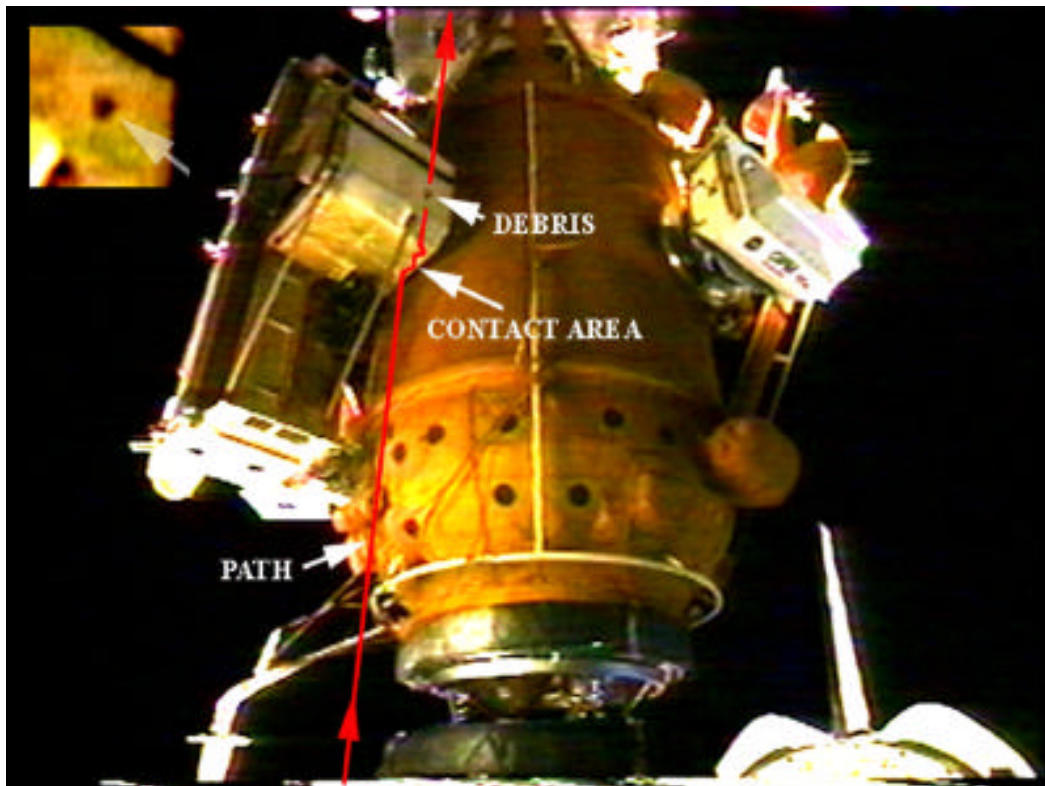


Figure 6.1 Debris Observed Making Contact with RSA Carrier at GMT 137d:02h:36m:28s

path is approximately 10.4 cm/sec. The component of velocity in the direction parallel to the X-axis of the video image plane changed from approximately 3.6 cm/sec to approximately 1.2 cm/sec. The diameter of the debris is approximately 4.3 cm. An examination of the film photography of the RSA carrier, taken while the Shuttle was docked, did not indicate any damage to the carrier thermal blanket as a result of the debris contact.

Three minutes and twenty-six seconds after the above debris was observed, a second piece of debris was observed as shown in Figure 6.2. This piece of debris was recorded by PLB camera C and traversed a path between PLB camera C and the Mir DM. This debris appears to be spherical in shape. The path of the debris indicates that the debris originated from the aft bulkhead area of the PLB. The distance of the debris from the camera cannot be determined and therefore the size and velocity of the debris cannot be determined.

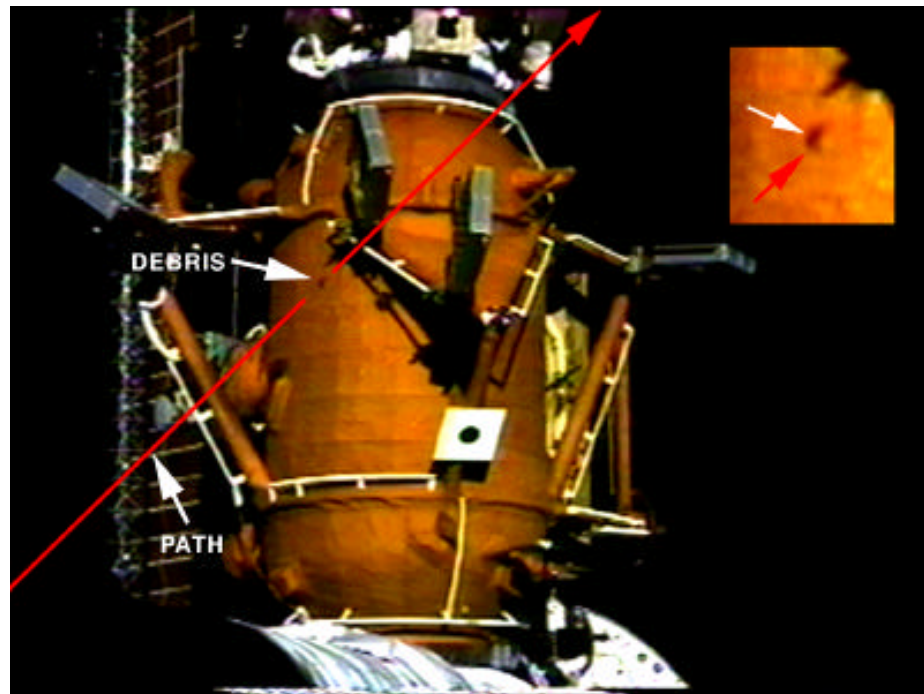


Figure 6.2 Spherical Debris Observed between PLB Camera C and Mir Docking Module at GMT 137d:02h:39m:54s

7. MIR ENVIRONMENTAL EFFECTS PAYLOAD ASSESSMENT

The Mir Environmental Effects Payload (MEEP) experiment was attached to the Mir Docking Module during STS-76. The four MEEP panels are shown as items 2-5 in Figure 2.2. The MEEP panels are scheduled to be retrieved on STS-86 (September 1997) and returned to the experimenters.

Figure 7.1 is an image of the Docking Module with MEEP experiment panels identified. The image was obtained during approach to Mir by the Orbiter using the 35 mm camera with 400 mm lens. This image and the image in Figure 7.2 shows the four panels to be in good condition. Comparisons with STS-76 images show the panels to be in their original installed orientations.

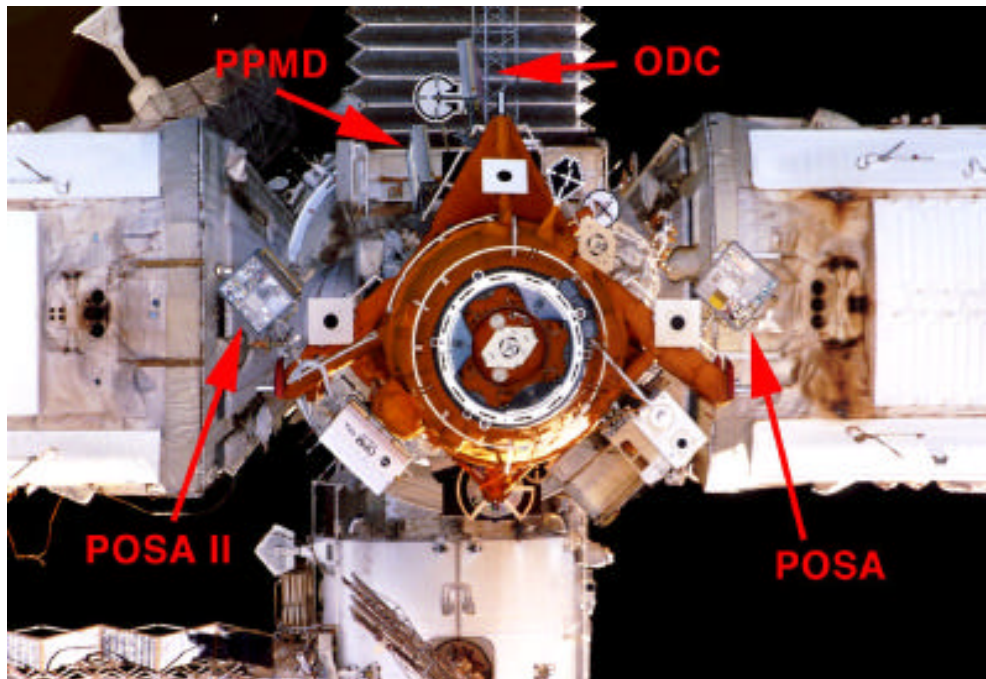


Figure 7.1. STS-84 Image of Mir with MEEP Experiments

Figures 7.2, 7.3, and 7.4 provide the highest quality images of the four MEEP experiments obtained on STS-84. The images have been digitally modified to the scale shown. There are no apparent damage or discolorations of any of the MEEP panels. Figure 7.2 is one of a set of images of POSA taken with the 35 mm camera and telephoto lens from the aft flight deck window. A small scratch which may be observed on the left two sections is attributed to a scratch on the film. Figure 7.3 shows the panels on both sides of POSA II. POSA II is the only experiment for which imagery was obtained of both sides of the experiment. The image on the left of Figure 7.3 (the POSA II side with the handle) was obtained with the 35 mm camera from the Spacehab window. The image on the right side was obtained during approach for docking. Both images are subsets from the original 35 mm frames. Figure 7.4 shows images of ODC and PPMD. The

image of PPMD was also taken from the Spacehab window and is the clearest image of PPMD obtained on any of the missions to date. The image of the ODC was acquired with the monochrome PLB camera B.

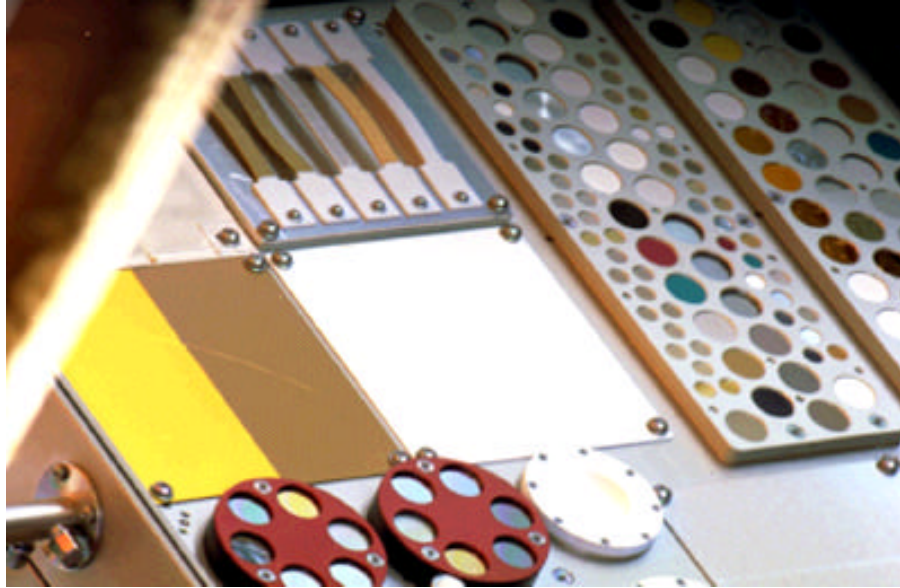


Figure 7.2 Image of POSA Acquired from Aft Flight Deck Window

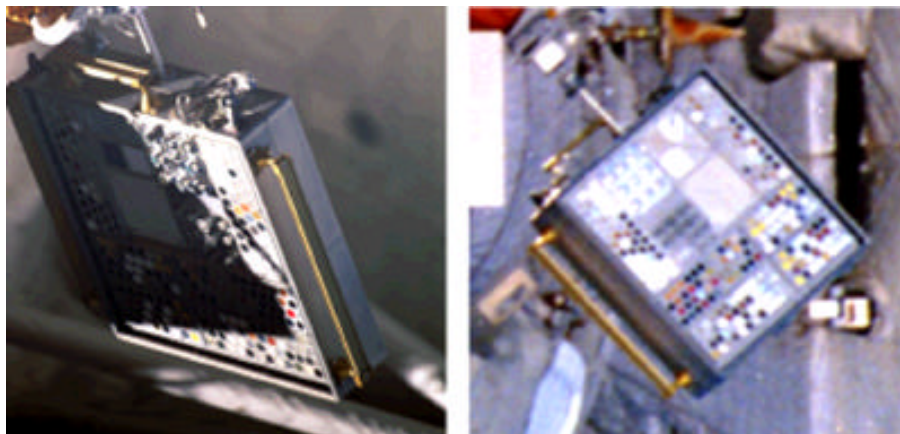


Figure 7.3 Images of Panels on Both Sides of POSA II

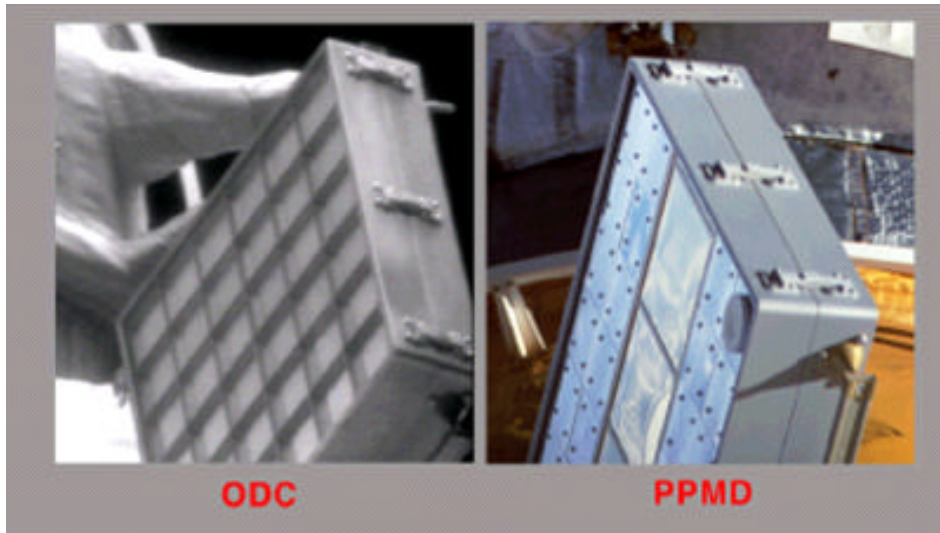


Figure 7.4 Images of ODC and PPMD

8. POSITION OF THE KURS ANTENNA ATTACHED TO THE DOCKING MODULE

Between STS-79 and STS-81, a Kurs antenna was attached to the Mir Docking Module. This Kurs antenna extends toward the Shuttle forward bulkhead as shown in Figure 8.1. The JSC Structures and Mechanics Division requested that an analysis be performed to determine the position of the tip of the antenna from STS-81 and STS-84 imagery. This information will assist the group in determining the clearances between the antenna and the Shuttle Payload Bay forward bulkhead. The STS-81 results were included in the DTO-1118 STS-81 Mission Report (JSC-27932). The following describes the STS-84 analysis and results.

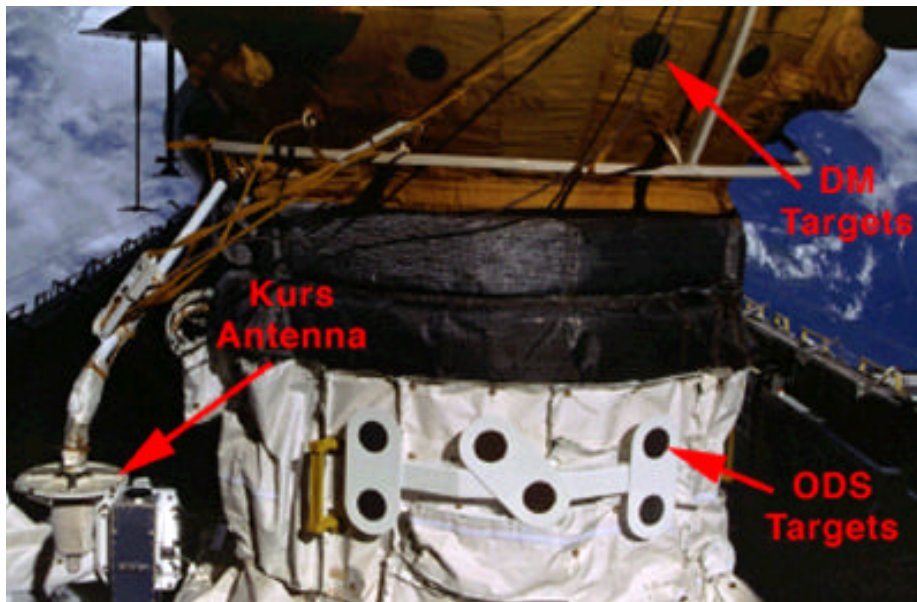


Figure 8.1 Kurs Antenna as seen from the Shuttle Flight Deck on STS-84

Standard photogrammetric techniques were used to determine the location of the Kurs antenna. The same techniques were used for both STS-81 and STS-84 analyses. Two overlapping images of the antenna were used to perform a 3-dimensional triangulation to determine the position of the tip of the antenna in the Shuttle Structural Coordinate System (SSCS).

Two STS-84 video images from Shuttle PLB cameras A and D were used in this analysis. These two images are shown as Figures 8.2 and 8.3, respectively. The ODS targets of the Orbiter Space Vision System (OSVS) were used to establish the camera pointing angles.

The results from the STS-84 analysis are given in Table 8-1. The STS-81 results and the expected coordinates based on data obtained from the Space Shuttle Program Integration Engineering Office are also in the table. The estimated positions from STS-81 and STS-

84 analyses are accompanied by an uncertainty estimate derived from a standard Monte Carlo error estimator. Both the STS-84 and STS-81 results indicate a clearance of 109 inches between the tip of the antenna and the Shuttle forward bulkhead.

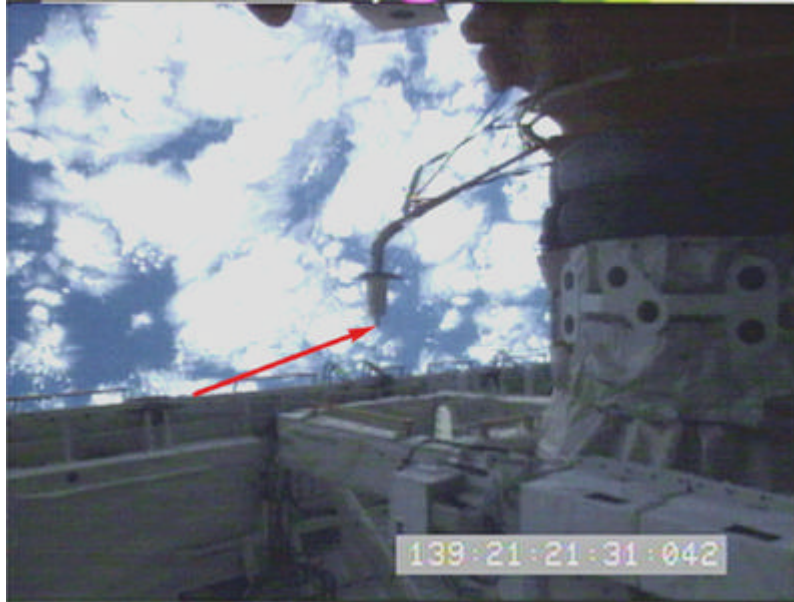


Figure 8.2 Kurs Antenna as seen from Payload Bay Camera A

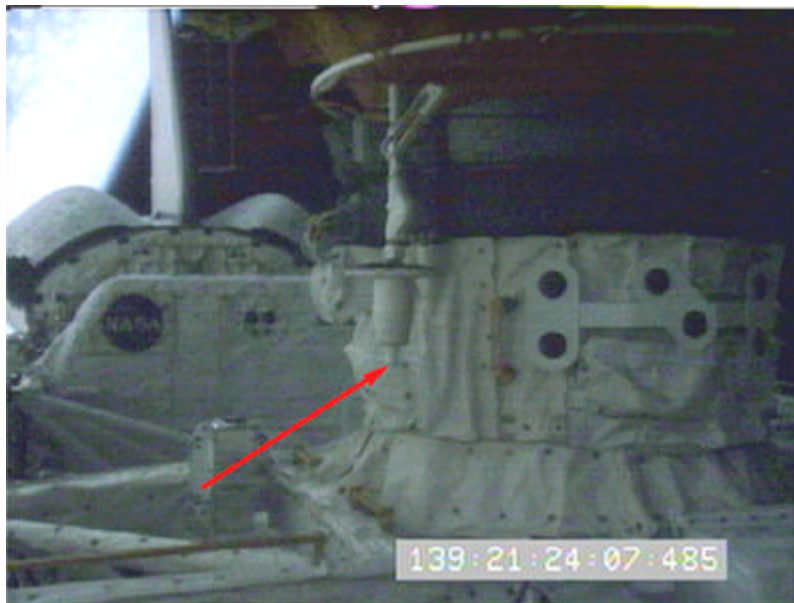


Figure 8.3 Kurs Antenna as seen from Payload Bay Camera D

Table 8-1 Coordinates of Kurs Antenna Tip

	SSCS Coordinates (inches)		
	$X_0 \pm 3\sigma$	$Y_0 \pm 3\sigma$	$Z_0 \pm 3\sigma$
Expected Position	683.4	40.5	439.1
STS-81 Position	685.5 ± 1.9	42.3 ± 1.1	439.3 ± 0.9
STS-84 Position	686.1 ± 1.6	40.5 ± 1.0	439.1 ± 0.9

The Monte Carlo analysis attempts to define the maximum expected deviation of the estimated position of the antenna tip from its true position. The primary contributors to the input errors are the errors in the digitized image positions of the tips. The resolution of the video imagery has a large effect on the ability to accurately establish the digital image positions, but resolution of a given image is affected by many contributing factors, many of which can not be accounted for in a simple Monte Carlo error analysis. Because of this, “worst case” variances are input to the Monte Carlo analysis which cause the results of the Monte Carlo error analysis to be overly conservative.

As an additional error assessment, the photogrammetric technique used to estimate the Kurs antenna position was also used to estimate the position of each of the six ODS targets. The ODS targets were also used to determine the pointing angles of the cameras for the photogrammetric solution. The results of these analyses were compared to the ground-surveyed positions of the ODS targets, which have a 1σ accuracy of ± 0.03 inches. The 3σ results of the differences between the estimated and surveyed positions of the ODS targets were: $3\sigma(X_0) = \pm 0.13$ inches; $3\sigma(Y_0) = \pm 0.17$ inches; $3\sigma(Z_0) = \pm 0.31$ inches. Comparison of these values with the error values for the position of the tip given in Table 8-1 implies the error values in Table 8-1 are conservative estimates of the true error.

9. IMAGERY EVALUATION

This section discusses the overall quality of the film and video data obtained during STS-84 for DTO-1118. The scenelist of flight films and an index to videotapes are included as Appendixes A and B. Appendix C is a list of image sources for the imagery in this report. Appendix D shows the configuration of STS-84 cameras.

Imagery acquired of Mir surfaces during STS-84 consisted of the following:

- Approximately 13 hours of downlink and onboard video.
- 830 frames of 35 mm film.
- 160 frames of 70 mm film.
- 7 Electronic Still Camera (ESC) images.

All DTO-1118 objectives and customer targets were obtained.

Use of the 2X teleconverter with the 400 mm lens provided excellent detailed photography during the docked phase of the flight. There was detail visible in this photography not captured on previous mission photography where the 250 mm, and only the 300 or 400 mm lens (without the teleconverter), was used. This additional detail is attributed to the increased magnification provided by the 2X lens. In addition to a review of the film and video, a summary of crew debrief comments are included.

9.1 Still Photography Review

Approximately 36 frames of Nikon (35 mm) photography were acquired during approach. These images, captured with a 400 mm lens, provided an overview of the Orbiter-facing sides of Mir modules. Three overview images of the Mir docking mechanism were acquired. Thirteen frames of Hasselblad (70 mm) photography were acquired during close approach. These images of the station were taken under poor lighting conditions since docking occurred at the end of a night pass. As on previous missions, limited overhead window access time during approach hampered data acquisition.

The STS-84 crew obtained large-scale, high-resolution photography of Mir surfaces while the Shuttle was docked. Imagery was taken from the Shuttle windows, the Spacehab window, and from Mir windows. This imagery was highly beneficial for analysis of MMOD strikes on portions of the Docking Module, Kvant-2 radiator, and the Base Block SP#2, Kristall SP#2, and Kvant-2 SP#2 solar arrays. Analyses of the sizes and numbers of MMOD strikes have not been performed on all the acquired imagery.

Overview coverage of the Orbiter-facing sides of Kvant, Spektr, Kvant-2, Kristall and Base Block modules was obtained using the Hasselblad camera during the docked phase. In addition, excellent detailed coverage of the following Docking Module features was acquired with the Nikon 35 mm camera:

- The newly deployed Optical Properties Monitor (OPM).

-
- Chipped paint on the Reusable Solar Array (RSA) carrier.
 - Deposition on the OPM thermal blankets.
 - The Remotely Operated Electrical Umbilical Payload Disconnect Assembly (ROEU PDA).
 - Chipped paint on handrails.
 - Possible debris strikes on the thermal blanket.
 - General thermal blanket discoloration.

Detailed coverage was also obtained of the Kvant end dome at the Base Block interface, the power cable running from SP #3 on the Base Block to the attach point of the CSA, experiments on the end of Kvant-2, the (-ZB) Spektr and Kvant-2 radiators, and the MEEP POSA panel.

Previously undetected MMOD strikes on the partially retracted Kristall (Solar Panel) SP #2 were visible in photography taken with the 400 mm lens. In addition, detailed views of the CSA, Kvant-2 SP #2, Base Block SP #2, and Kvant SP #1 were acquired.

Overview photography of the Station was obtained with both the Nikon and Hasselblad cameras during backaway. Limited overhead window access time hampered image acquisition, however some overview photographs of the Station were taken with both the Nikon and Hasselblad cameras.

Electronic Still Camera (ESC) imagery of Mir provided seven views of Mir during approach. These represented the only ESC frames taken of the external surface of Mir.

STS-84 was the first Shuttle/Mir mission that did not have a fly-around of the Mir by the Shuttle. Additionally, close-up photographs of Mir taken during Shuttle approach were obtained during poor lighting conditions and there were no close-up photographs taken during back-away. Therefore the amount of high-resolution photographic coverage of Mir was greatly reduced from the previous missions.

9.2 Video Review

Payload bay camera A and the ODS centerline camera provided the first views of the Mir approximately 1 hour before docking. During the dark phase of the orbit, only the station onboard lights were visible on the available views.

Final approach and docking occurred during darkness. The OSVS targets and the DM docking target were visible in the ODS centerline camera during the docking sequence. Limited detail could be observed on the docking mechanisms due to glare reflected from the docking ring caused by the docking lights. However, the video during docking and backaway was sufficient to show the docking target in excellent condition and the capture and structural latches in proper position. The electrical connectors and laser retroreflectors appeared to be in good physical condition. None of the mission imagery was sufficient to evaluate deposition/discoloration of the docking surfaces.

PLB camera A recorded images of a piece of debris three seconds after Mir capture and PLB camera C captured a second piece three seconds later. PLB camera B was pointed

toward space for a few minutes during distant approach to Mir and over 100 pieces of orbital debris was counted. Camera B was the low light level, monochromatic camera.

PLB camera C had a smudge on the lens which affected image data quality. During the early portions of the flight through the docking phase, the video image appeared clear. Video scenelisters noted a “spot of moisture condensate on the lens” at GMT 137d:16h:33s:36f. This was approximately 14 hours after Mir contact and capture. Four hours after the spot was noted, it had become a smudge on the center of the lens and remained a large smudge for the duration of the Mir surveys. This smudge significantly affected survey imagery because of the size of the smudge and the fact that the center of the lens is the target point for most features to be imaged.

PLB camera B also had a few small spots which may have been debris attached to the front of the lens. These spots on PLB camera B did not significantly affect survey image quality.

An INCO-controlled video survey was performed during two crew sleep periods of the docked phase. All four payload bay cameras were used in acquiring Mir survey imagery. This footage provided good coverage of the Orbiter-facing sides of the Spektr, Kvant-2, Base Block, Kristall, Kvant, Priroda, Soyuz and Progress modules. In addition, systematic coverage of the Docking Module and the attached RSA carrier was obtained. Coverage was also obtained of the newly-deployed OPM experiment mounted on the Docking Module. The use of cameras B and C during the INCO survey was limited.

Video mapping of solar array surfaces on Mir was undertaken during the INCO survey. The solar array attach points were also covered. Controlled opening and closing of the payload bay camera iris optimized the quality of video images for extraction of information about the condition of the solar array attach points.

The Mir Structural Dynamics Experiment (MiSDE) was performed during the docked portion of STS-84. During Shuttle thruster firings, payload bay cameras A and D were multiplexed, and recorded motion at the tip of Base Block SP#2 while cameras B and C recorded motion at the array attach. Video obtained during MiSDE test firings was of acceptable quality for analysis.

9.3 Crew Assessments

The following is a summary of STS-84 crew assessment of the imagery acquisition. The summary is based on a debrief held on June 13, 1997.

- Preflight training was adequate to perform the DTO (two training sessions were held: familiarization and detailed).
- Additional charts, handouts, and photos would be helpful for the crew to locate desired target areas. A list of photos based on location and priority would also be beneficial.
- Additional mission time should be scheduled for the DTO. The crew took photography during the allocated sessions in the mission timeline, however the crew also requested and received an additional session for photography during the STS-84 mission. The crew felt that more film should be manifested for the DTO.

-
- The physical locations of some of the windows, coupled with the size of the camera equipment, made photography difficult from Mir windows, especially Kvant-2.
 - During approach and backaway, it was difficult to acquire targets due to poor lighting and limited overhead window access time.

10. CONCLUSIONS AND RECOMMENDATIONS

10.1 Conclusions

Based on the analysis of STS-84 imagery, the following conclusions have been made:

- Photography and video acquired during STS-84 provided valuable results important to the success of Shuttle/Mir missions and International Space Station developers. Specifically, this included the areas of loads and dynamics, structures and mechanisms, contamination of materials and coatings, micrometeoroid and orbital debris modeling, payloads, and operations.
- The imagery from the STS-84 mission substantially augmented the imagery from previous Shuttle/Mir missions. The combined imagery gathered on STS-63 through 84 missions provide significant information from which assessments can be made about the effects of the space environment on an orbiting platform.
- The amount of high-resolution imagery continues to increase with each additional mission. Although major Mir surface changes were not observed on STS-84, there is improved identification of smaller features and definition of surface characteristics, including discoloration, micrometeoroid/orbital debris damage, and surface and structural anomalies.
- Imagery over several missions is critical to the analyses. New details are revealed with each mission. Changes can be tracked and results can be corroborated. Determination of the number, locations, and sizes of MMOD strikes required the imagery of different scales, resolutions, and viewing perspectives from a multiple number of missions.

10.2 Recommendations

Based on the summary above, crew comments during training and post-mission debriefs, and evaluation of the STS-84 and prior mission imagery, the following recommendations are made for upcoming Shuttle/Mir and ISS missions:

- High resolution imagery of the Spektr radiator should continue to be acquired for each mission for purposes of monitoring the leak in the radiator.
- The Nikon with 400 mm lens should be the primary source for survey imagery acquisition. The higher resolution of this system provides greater detail of information during approach, while the Orbiter is docked, during backaway, and during fly-around.
- Centerline video camera views should be the primary source for determining the condition of the centerline docking target. However, for docking mechanism assessment, crew time should continue to be provided for acquisition of close-up film imagery. STS-81 imagery using the Nikon with the 180 mm lens demonstrated the value of close-up imagery. Additional options for improving docking mechanism imagery include: use of the 400 mm lens, improved lighting and vehicle orientation, changing the timelines for docking and backaway, improved imagery equipment, and station-keeping at close range after backaway.

-
- If imagery is to be obtained of the Docking Module electrical connectors, consideration should be given to using the Nikon with the 400 mm lens during close approach and backaway in the range of 30 to 60 feet. The 180 mm lens was used during STS-81 to great benefit, however the 400 mm lens should double the resolution.
 - An updated mission-specific target priority list should continue to be generated for the crew at the last training session. The target priorities change based upon modifications to the Mir configuration, late-developing target requirements, Shuttle camera changes, and operations planning.
 - INCO-controlled payload bay video cameras should continue to be used to perform Mir surveys during crew sleep periods. This has been the most effective way to obtain survey video coverage and also allows real-time decisions to be made on target acquisition.
 - The need for bracketing exposures when acquiring imagery should continue to be emphasized. The bracketed exposures provide for additional detail in the imagery not obtained with a single exposure.
 - The crew should continue to be made aware of lighting conditions that highlight surface features. Lighting angles oblique to Mir surfaces convey textural information that would otherwise remain hidden.

11. REFERENCES

1. NASA/RSC-E Joint Report, Mir Photo/TV Survey (DTO-1118): STS-63, JSC-27246, August 28, 1995.
2. NASA/RSC-E Joint Report, Mir Photo/TV Survey (DTO-1118): STS-71, JSC-27355, January 16, 1996.
3. NASA/RSC-E Joint Report, Mir Photo/TV Survey (DTO-1118): STS-74, JSC-27649, November 20, 1996.
4. Mir Photo/TV Survey (DTO-1118): STS-76 Mission Report JSC-27525, July 30, 1996.
5. Mir Photo/TV Survey (DTO-1118): STS-79 Mission Report JSC-27761, March 28, 1997.
6. Mir Photo/TV Survey (DTO-1118): STS-81 Mission Report JSC-27932, July 11, 1997.
7. Kerslake, Thomas W., Lewis Research Center, Personnel communication, September 1997.
8. Christiansen, Eric, Johnson Space Center, Personnel Communication, September 1997.

12. ACRONYMS & ABBREVIATIONS

CCD	Charge Coupled Device
CLTV	Centerline TV
CSA	Cooperative Solar Array
CTVC	Color Television Camera
DM	Docking Module
DTO	Detailed Test Objective
ESC	Electronic Still Camera
EVA	Extra Vehicular Activity
FFT	Fast Fourier Transform
GMT	Greenwich Mean Time
INCO	Instrumentation and Communication Officer
ITVC	Intensified TV Camera
IS&AG	Image Science & Analysis Group
ISS	International Space Station
JSC	Johnson Space Center
LeRC	Lewis Research Center
LMES	Lockheed Martin Engineering and Sciences
MEEP	Mir Environmental Effects Payload
MiSDE	Mir Structural Dynamics Experiment
NASA	National Aeronautics & Space Administration
ODC	Orbital Debris Collector
ODS	Orbiter Docking System
OPM	Optical Properties Monitor
OSVS	Orbiter Space Vision System
PDA	Payload Disconnect Assembly
PLB	Payload Bay
PPMD	Polished Plate Micrometeoroid & Debris
POSA	Passive Optical Sample Assembly
POSA II	Passive Optical Sample Assembly II
ROEU	Remotely Operated Electrical Umbilical
RSA	Reusable Solar Array
SA	Solar Array
SP	Solar Panel
SSCS	Space Shuttle Coordinate System
STS	Space Transportation System

Appendices

Appendix A: STS-84 Film Scenelist

Appendix B: STS-84 Video Scenelist

Appendix C: Sources for Report Imagery

Appendix D: STS-84 Camera Layout

Appendix A: STS-84 Film Scenelist

The attached STS-84 film scenelist was compiled by the Imagery and Publications Office/BT4 and breaks down coverage of items on each roll of 35 mm and 70 mm film.

Table A-1 Still Photography Coverage of Mir Rendezvous Events

	Approach	Docked (survey)	Backaway
Hasselblad (Roll #)	730	702, 704, 709, 722, 723, 724, 727, 729, 730, 731,	708
Nikon (Roll #)	350	303, 309, 322, 328, 329, 330, 331, 332, 333, 334, 338, 339, 340, 341, 342, 343, 345, 346, 347, 348, 352, 353, 357, 358, 374, 378, 380	322
ESC	S84E5001, S84E5002, S84E5003, S84E5004, S84E5005, S84E5006, S84E5007	S84E5089, S84E5244	

The above table summarizes the event coverage recorded by the different still photography sources. Note that the specified rolls contain additional images unrelated to the Mir survey.

STS-84 Flight Film Contents Organized by Category, Roll, and Frame

Mag	Frames	Count	Film	Description
Category: Prime Mission Obj.				
E	5001 thru 5007	7	DIG. FILE	Mir space station views during docking operations on STS-84
	5089 thru 5089	1	DIG. FILE	Spektr solar array panels as seen from the shuttle flight deck window
303	005 thru 007	3	35MM	View of the Mir space station from the forward Spacehab window
	010 thru 010	1	35MM	View of the Mir space station from the forward Spacehab window
	012 thru 030	19	35MM	View of the Mir space station from the aft Spacehab window
	033 thru 037	5	35MM	Transfer ops documented in the Spacehab module
306	037 thru 037	1	35MM	View of Mir Space Station as seen from flight deck overhead window
309	001 thru 014	14	35MM	View of Mir Space Station as seen from flight deck overhead window and Spacehab
310	020 thru 026	7	35MM	Mir space station as viewed through the flight deck window COAS
322	001 thru 023	23	35MM	Views of Mir Space Station after undocking and during separation
328	001 thru 038	38	35MM	DTO 1118 - Mir survey
329	001 thru 037	37	35MM	DTO 1118 - Mir survey
330	001 thru 037	37	35MM	DTO 1118 - Mir survey
331	001 thru 036	36	35MM	DTO 1118 - Mir survey
332	001 thru 037	37	35MM	DTO 1118 - Mir survey
333	001 thru 037	37	35MM	DTO 1118 - Mir survey
334	001 thru 037	37	35MM	DTO 1118 - Mir survey
338	001 thru 037	37	35MM	DTO 1118 - Mir survey
339	001 thru 037	37	35MM	DTO 1118 - Mir survey
340	001 thru 037	37	35MM	DTO 1118 - Mir survey
341	001 thru 037	37	35MM	DTO 1118 - Mir survey
342	001 thru 038	38	35MM	DTO 1118 - Mir survey
343	001 thru 038	38	35MM	DTO 1118 - Mir survey
345	001 thru 037	37	35MM	DTO 1118 - Mir survey
346	001 thru 037	37	35MM	DTO 1118 - Mir survey
347	001 thru 035	35	35MM	DTO 1118 - Mir survey
348	001 thru 037	37	35MM	DTO 1118 - Mir survey
350	001 thru 036	36	35MM	Views of the Mir Space Station during rendezvous
352	001 thru 037	37	35MM	DTO 1118 - Mir survey
353	001 thru 037	37	35MM	DTO 1118 - Mir survey
357	026 thru 026	1	35MM	View of the Mir Space Station during docked operations
	033 thru 037	5	35MM	View of the Mir Space Station during docked operations
377	012 thru 012	1	35MM	View looking along Kristall module as seen from the shuttle flight deck
378	001 thru 004	4	35MM	View of the Mir Space Station framed by an overhead flight deck window
	021 thru 023	3	35MM	View of the Mir Space Station DM framed by an aft flight deck window
380	029 thru 031	3	35MM	View of the Mir Space Station taken from the Spacehab view port
702	032 thru 032	1	70MM	Mir Space Station Spektr solar array
704	000AK thru 000AK	1	70MM	Partial view of both Progress supply ship and Cooperative Solar Array
708	051 thru 066	16	70MM	Overall of the Mir Space Station during separation after undocking
712	015 thru 015	1	70MM	View of the Mir Space Station Base Block and window in shadow
722	094 thru 096	3	70MM	Mir Space Station Base Block and Kvant exterior, backdropped by Earth limb
723	001 thru 004	4	70MM	Kvant-2 module with Russian Manned Maneuvering Unit (MMU) in stowed position
	095 thru 098	4	70MM	Kvant, Base Block and Kristall exteriors over the Earth limb
727	011 thru 013	3	70MM	Russian MMU stowed on end of Kvant-2 module
729	041 thru 044	4	70MM	Attitude control thruster boom on Mir Space Station
730	001 thru 013	13	70MM	Mir survey just before docking
	021 thru 052	32	70MM	Survey of the Mir Space Station including the OPM hardware
731	025 thru 068	44	70MM	Survey of Mir Space Station solar arrays

Appendix B: STS-84 Video Scenelist Information

Table B-1 Video Coverage of Mir Rendezvous Events

	Approach	Docked (Survey)	Backaway
Downlink (reel #)	13, 15	16, 24, 25, 26, 27, 28, 29, 30, 41	41, 42
Onboard (tape ID #)	22, 30, 31, 36	18, 21	20, 26

The above table summarizes the event coverage recorded onto the different downlink and onboard tapes. Note that some of the downlink scenes may be overlapped by those on the onboard video.

A scenelist is available for each shuttle mission, STS-1 through the present. Copies of these may be requested at the Imagery & Publications Office Customer Service Desk, mail code BT4, Johnson Space Center, Houston, Texas. Phone: (713) 483-7777.

SCENELIST GUIDE

A Scenelist is a written account of all video recorded during a shuttle mission. It identifies the action taking place on the video, the corresponding videotape number of the recorded video.

There are four main divisions of mission video: Launch, Downlink, Onboards, and Landing. These divisions are identified in the scenelist

Launch and landing video are recorded from the NASA Select satellite transmission which originates from the Kennedy Space Center or Edwards Air Force Base landing, depending upon the landing site.

Downlink video is transmitted through the Tracking and Data Relay Satellite System, or TDRSS, to Johnson Space Center where it may be sent from the orbiter live as it occurs (real time), or it may be recorded by the crew and relayed down as a VTR playback.

Onboard video is recorded by the crew during the mission using a 3/4 inch or 8mm tape format. This video is transferred, post-mission, for storage and archival purposes.

In each Scenelist heading there are four areas of information: The master tape number, title, GMT and MET days, and the Caption.

The tape number is the number of the master recording of the video scenelisted on that page.

The title notates the mission and the segment of video scenelisted on that page, ex: STS-84 Downlink Orbits 002, 003 or STS-84

The GMT and MET days are part of the time code track that is recorded along with the mission video. This time code is a label for to tell where a particular scene is located on a master recording. In the scenelist heading three time codes are referenced. They are GMT, Mission Elapsed Time or MET, and the Society of Motion Picture and Television Engineers time code, or SMPTE. Also GMT and MET are noted. This Event GMT and MET tell when the video was actually recorded on-orbit whereas the "real time" C was downlinked (sent) to Earth. The SMPTE time code is used to identify where a scene may be found on a master tape. This is used when requesting video. On downlink video the GMT and SMPTE time code are identical so only one time code is referenced, this is the GMT and SMPTE differ, so both time codes are referenced. Most video recorded with a camcorder does not have GMT so the time unless an audio cue is given. These audio cues are included in the scenelist.

The caption lists the major subjects or events in the section of video scenelisted underneath the heading. It also notates the type of

A sample of the scenelist headings are shown on the next page.

Appendix C: Sources for Report Imagery

<u>Figure #</u>	<u>Caption</u>	<u>Photograph / Tape #</u>
	Cover Photograph	STS084-303-021
Figure 2.1	Mir Space Station	STS084-350-011
Figure 2.2	Docking Module	STS084-350-023
Figure 3.2	Kristall SP#2 MMOD Strikes	STS084-342-036
Figure 3.3	Base Block SP#2 MMOD Strikes	STS084-340-033
Figure 3.4	Circular MMOD Strike Pattern on Base Block SP#2	STS084-339-026
Figure 3.5	MMOD Strikes on Kvant-2 SP#2	STS084-332-034
Figure 3.6	A View of the Back Side of Kvant-2 SP#2 MMOD Strike	STS071-703-018
Figure 3.7	Possible MMOD Strikes on a Portion of Kvant-2 Radiator	STS084-332-034
Figure 3.8	Possible MMOD Strikes on Docking Module Thermal Blanket	STS084-328-014
Figure 3.9	Deposition on Base of RSA Carrier	STS084-328-001
Figure 3.10	Irregularity on Surface of an RSA Carrier Hinge	STS084-328-004
Figure 3.11	Discoloration and Possible Stain on Docking Module Thermal Blanket	STS084-328-016
Figure 3.12	Docking Module - ROEU-PDA	STS084-330-012
Figure 3.13	Docking Module - OPM	STS084-730-025
Figure 3.14	Progress of Possible Leak on Spektr Radiator	STS079-305-012 STS081-333-020 STS081-332-004
Figure 4.1	Photo of Docking Mechanism during Approach	STS084-350-023
Figure 4.2	Video of Docking Mechanism during Backaway	Tape #613911
Figure 5.1	A Multiplexed Video Frame Used in the Motion Analysis of Base Block SP#2	Tape #613869
Figure 6.1	Debris Observed Making Contact with RSA Carrier	Tape #613937
Figure 6.2	Spherical Debris Observed between PLB Camera C and Mir Docking Module	Tape #613937
Figure 7.1	STS-84 Image of Mir with MEEP Experiments	STS084-350-023
Figure 7.2	Image of POSA Acquired from Aft Flight Deck Window	STS084-330-027
Figure 7.3	Images of Panels on Both Sides of POSA II	STS084-343-025 (left) STS084-343-023 (right)
Figure 7.4	Images of ODC and PPM D	Tape #613899 (left) STS084-346-028 (right)
Figure 8.1	Kurs Antenna as seen from the Shuttle Flight Deck on STS-84	STS084-358-022
Figure 8.2	Kurs Antenna as seen from Payload Bay Camera A	Tape #613900
Figure 8.3	Kurs Antenna as seen from Payload Bay Camera D	Tape #613900

Appendix D: STS-81 Camera Layout

The following diagram depicts the layout of film and photographic equipment specific to Mir survey events during the STS-84 rendezvous.

STS-84 Shuttle / MIR

SURVEY CAMERA SETUP

